A reinterpretation of the Navado-Filábride and Alpujárride Complexes (Betic Cordillera) : field, petrography and U-Pb ages from orthogneisses (western Sierra Nevada, S Spain)

Autor(en): **Gómez-Pugnaire, M.T. / Galindo-Zaldívar, J. / Rubatto, D.**

Objekttyp: **Article**

Zeitschrift: **Schweizerische mineralogische und petrographische Mitteilungen = Bulletin suisse de minéralogie et pétrographie**

Band (Jahr): **84 (2004)**

Heft 3

PDF erstellt am: **25.09.2024**

Persistenter Link: https://doi.org/10.5169/seals-63751

Schweizerische Mineralogische und Petrographische Mitteilungen 84, 303–322, 2004

A reinterpretation of the Nevado-Filábride and Alpujárride Complexes (Betic Cordillera): field, petrography and U–Pb ages from orthogneisses (western Sierra Nevada, S Spain)

M.T. Gómez-Pugnaire[1], *J. Galindo-Zaldívar*[2], *D. Rubatto*[3], *F. González-Lodeiro*[2], *V. López Sánchez-Vizcaíno*[4] and *A. Jabaloy*[2]

Abstract

We investigated gneisses from the upper sequence of the Nevado-Filábride Complex in the western Sierra Nevada, close to the contact with the Permo-Triassic Alpujárride Complex. Despite intense deformation, the occurrence of skarn-like lenses (epidote + amphibole + garnet + quartz) and abundant post-magmatic hydrothermal tourmaline in both the gneisses and adjacent metasediments strongly suggests that an originally intrusive contact is preserved. High-pressure assemblages are not preserved in the dated gneisses due to intense retrograde overprinting during exhumation. Nevertheless, thermobarometry performed in adjacent skarn rocks and metapelites indicates maximum temperatures and pressures ranging from 605 ± 74 to 715 ± 72 °C and from 11.0 ± 2.5 to 14.5 ± 2.5 kbar. SHRIMP ion microprobe U–Pb analyses were performed on zircons from one gneiss. The zircon crystals display igneous oscillatory-zoned domains, with an age of 301 ± 7 Ma (95% c.l.), rimmed by dark, unzoned overgrowths of metamorphic origin (mean age of 16.5 ± 0.4 Ma). The former age is interpreted as dating the crystallisation of the granitic protolith of the gneiss. This implies a pre-Permian age for the Nevado-Filábride marbles, traditionally considered to be Triassic, and a Palaeozoic age for the complete sequence of the upper part of the Complex. Accordingly, in western Sierra Nevada, the observed succession from the Nevado-Filábride Complex to the Alpujárride Complex (Permo-Triassic phyllites and Triassic marbles) can be considered normal from a stratigraphic point of view. Therefore, the present-day contact between the two complexes, the Mecina Fault in Sierra Nevada, is interpreted as a normal fault generated during exhumation rather than a thrust structure.
The age of the metamorphic zircon overgrowths (16.5 ± 0.4 Ma) is likely to be related to decompression, as suggested by titanite inclusions found in zircon. Titanite postdates rutile, the high-pressure Ti-rich phase. This indicates exhumation of the Nevado-Filábride Complex significantly after the Alpujárride Complex (~18 Ma).

Keywords: Zircon, SHRIMP U–Pb geochronology, high-pressure metamorphism, Hercynian magmatism, Betic Complexes.

Introduction

Since the earliest studies on the Betic Cordillera (Brouwer, 1926; Staub, 1934; Fig. 1) the Internal Zones are subdivided into three main tectonic complexes called, from bottom to top, Nevado-Filábride, Alpujárride and Maláguide Complexes.

In particular, the separation of the Alpujárride and Nevado-Filábride into two tectonic complexes has been based on several (i) lithostratigraphic, (ii) metamorphic and, (iii) tectonic hypotheses.

(i) It has been proposed (Fallot, 1948; Fallot et al., 1961; Egeler and Simon, 1969, among many others) that the two complexes are composed of Palaeozoic lower series, which underwent pre-Alpine metamorphism, and of Mesozoic upper rocks, affected by Alpine metamorphism only. However, there are no reliable data about the age of the protoliths, or the age of metamorphism.

Additionally, a common sedimentary evolution has been assumed for the Mesozoic rocks in the Alpujárride and Nevado-Filábride Complexes (Egeler and Simon, 1969). In fact, Permo-Triassic (and younger, Tendero et al., 1993) ages were inferred for the upper rocks of the Nevado-Filábride Complex (Nijhuis, 1964), based on the litho-

[1] Departamento de Mineralogía y Petrología, Facultad de Ciencias, Universidad de Granada, Fuentenueva, s/n 18002 Granada, Spain. <teresa@ugr.es>
[2] Departamento de Geodinámica, Facultad de Ciencias, Universidad de Granada, Fuentenueva, s/n 18002 Granada, Spain.
[3] Research School of Earth Sciences and Department of Geology, Australian National University, Canberra ACT 0200, Australia.
[4] Departamento de Geología, E.U. Politécnica de Linares, Universidad de Jaén, Alfonso X el Sabio 28, 23700 Linares, Spain.

0036-7699/04/0084/303

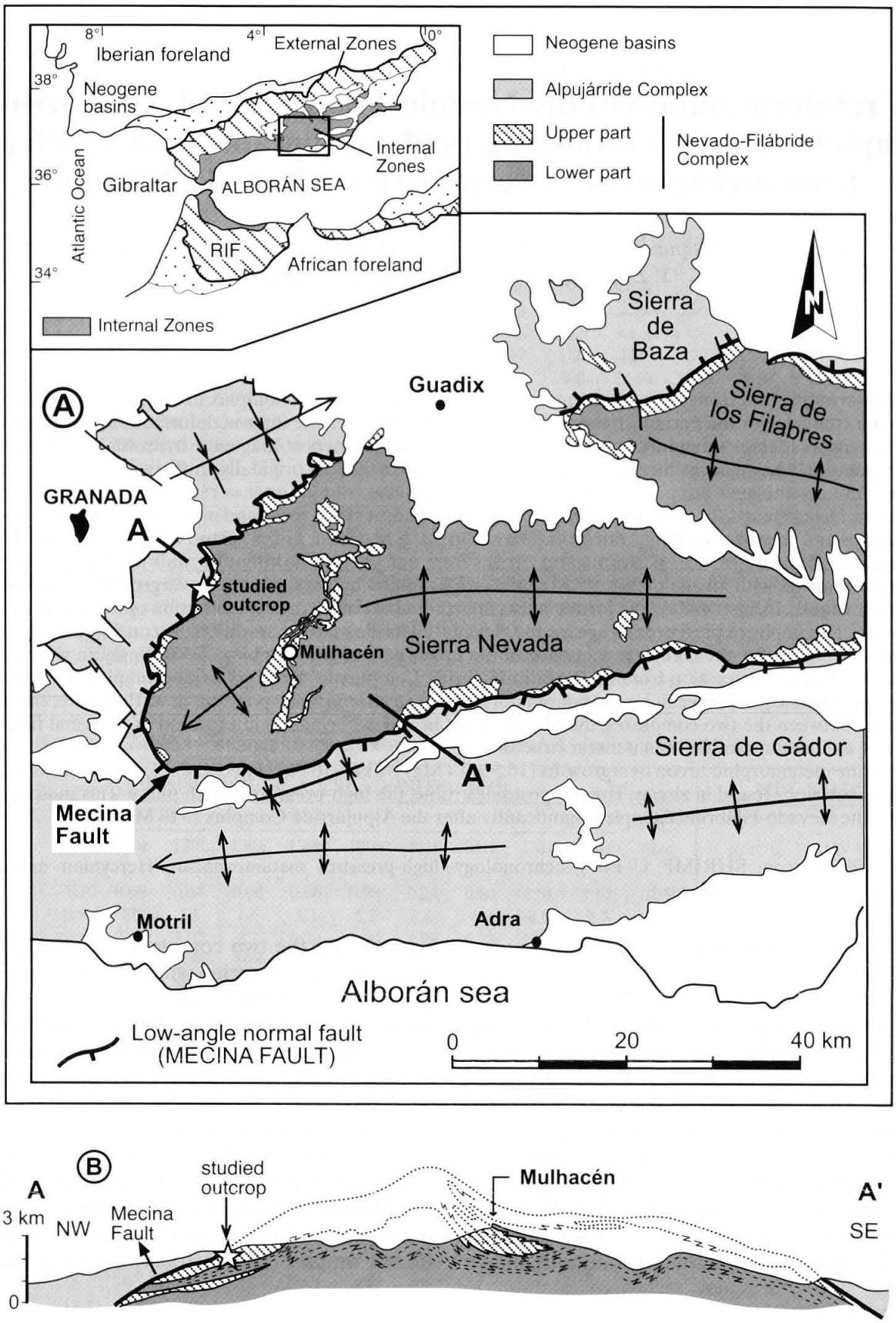

Fig. 1 Geological setting of the dated gneisses outcrop. (A) Tectonic sketch map of the western Sierra Nevada (Internal Zones). (B) Cross-section shown in A.

logical correlation with the overlying Alpujárride phyllites and carbonates dated with fossils (Barrois and Offert, 1889; Martín and Braga, 1986; Braga and Martín, 1987). This correlation has been upheld in most of the models and interpretations of the geological evolution of the Betic Cordill-

eras (see revision in Azañón et al., 2002 and references therein).

(ii) Different metamorphic conditions have been attributed to the Alpine metamorphism affecting the two complexes. The Nevado-Filábride rocks underwent high-pressure metamorphism (e.g. De Roever and Nijhuis, 1963; Nijhuis, 1964; Puga, 1976; Gómez-Pugnaire, 1982; Vissers, 1981; Bakker et al., 1989; De Jong, 1991). In contrast, low- to intermediate-pressure conditions were estimated for the overlying Alpujárride rocks (e.g., Westra, 1969; Torres-Roldán, 1979; Akkerman et al., 1980).

(iii) The tectonic contact between the Nevado-Filábride and the lowermost units of the Alpujárride Complex has been interpreted as a post-metamorphic thrust structure, based mostly on (i) and (ii).

Different lines of evidence indicate the weakness of the above hypotheses.

(a) The sedimentary evolution of the Mesozoic Alpujárride sequences is substantially different from the one of the Nevado-Filábride sequences, as demonstrated by De Jong and Bakker (1991) and Gómez-Pugnaire et al. (2000), making any subsequent lithostratigraphic correlation questionable. In addition, Rb–Sr data on gneisses from Sierra de los Filabres suggest a Palaeozoic age for the entire succession of the Nevado-Filábride Complex (Gómez-Pugnaire et al., 2000).

(b) Recent studies demonstrate that the Alpine metamorphic evolution seen in the Mesozoic rocks of the Alpujárride Complex is comparable to that of the Nevado-Filábride and coherent with the present relative position of both complexes. High-pressure assemblages found in the Alpujárride Complex (Goffé et al., 1989; Azañón, 1991, in the lower units around the Nevado-Filábride Complex; Tubía and Gil Ibarguchi, 1991, in the upper units) allowed Gómez-Pugnaire et al. (2000, see their Fig. 5) to deduce a common metamorphic field gradient for the two complexes. The lower pressure and temperature values of the Alpujárride rocks with respect to the Nevado-Filábride Complex are in agreement with the higher crustal location of the former complex during the metamorphic overprint (De Jong, 1991).

(c) The extensional character of the Nevado-Filábride/Alpujárride contact, which has been reinterpreted as a post-metamorphic extensional detachment (Fig. 1, Galindo-Zaldivar et al., 1989; Platt and Vissers, 1989).

The debate on these issues indicates that the current interpretation of the relationships between the Nevado-Filábride and Alpujárride Complexes needs revision. Improved geochronology on the protoliths and the understanding of the metamorphic evolution followed by the rock sequences in the two complexes are necessary for this revision.

In this contribution we report the first ion microprobe (SHRIMP) U–Pb ages on zircon crystals from one gneiss of the Nevado-Filábride Complex from western Sierra Nevada (Fig. 1). The gneisses, which appear in the highest part of the Nevado-Filábride Complex show the same deformation and underwent the same early high-pressure metamorphic event as the surrounding metasediments. Furthermore, we show the effect of contact metamorphism and hydrothermal activity related to the gneiss bodies which indicate an original intrusive emplacement. The radiometric ages obtained constrain the minimum ages of country rocks, and hence the age of the whole Nevado-Filábride Complex, and the age of the metamorphism. The results confirm and refine the previously proposed Palaeozoic age for the complex (Gómez-Pugnaire et al., 2000). On the basis of our new radiometric and thermobarometric data we discuss the reliability of the hypothesis supporting the separation of the Alpujárride and the Nevado-Filábride sequences in two different complexes. The Palaeozoic age of the dated sampled supports a stratigraphic relationship between both complexes: the Nevado-Filábride represents a Palaeozoic substrate (pre-Alpine basement) upon which the Permo-Triassic phyllites and marbles Alpujárride around Sierra Nevada (cover) were deposited.

Geological Setting

The Nevado-Filábride Complex is divided into two lithological units (Fig. 2). The lower unit (A in Fig. 2) mainly consists of a (>2 km) thick and monotonous sequence of graphite-bearing metapelites with intercalated quartzites and scarce graphite-bearing marbles (up to 1 m thick). This unit constitutes more than 90% of the outcrops in the western part of Sierra Nevada. This lower unit has been assumed to be Palaeozoic or older in age on the basis of the occurrence of a few Middle Devonian (Lafuste and Pavillon, 1976) and Pre-Cambrian (Gómez-Pugnaire et al., 1982) fossils in marbles and metapelites. Ages of metagranitic bodies intruded in the graphite-bearing metasediments (Fig. 3) range from 307 ± 34 Ma (Sm/Nd, Nieto et al., 1997) to 269 ± 6 Ma (Rb–Sr whole-rock, Priem et al., 1966; Andriessen et al., 1991). They indicate a Late Carboniferous to Late Permian age for both the host rocks and the metagranites.

This Palaeozoic and Pre-Cambrian lower part of the Nevado-Filábride Complex is overlain by light-coloured metasediments, up to several hun-

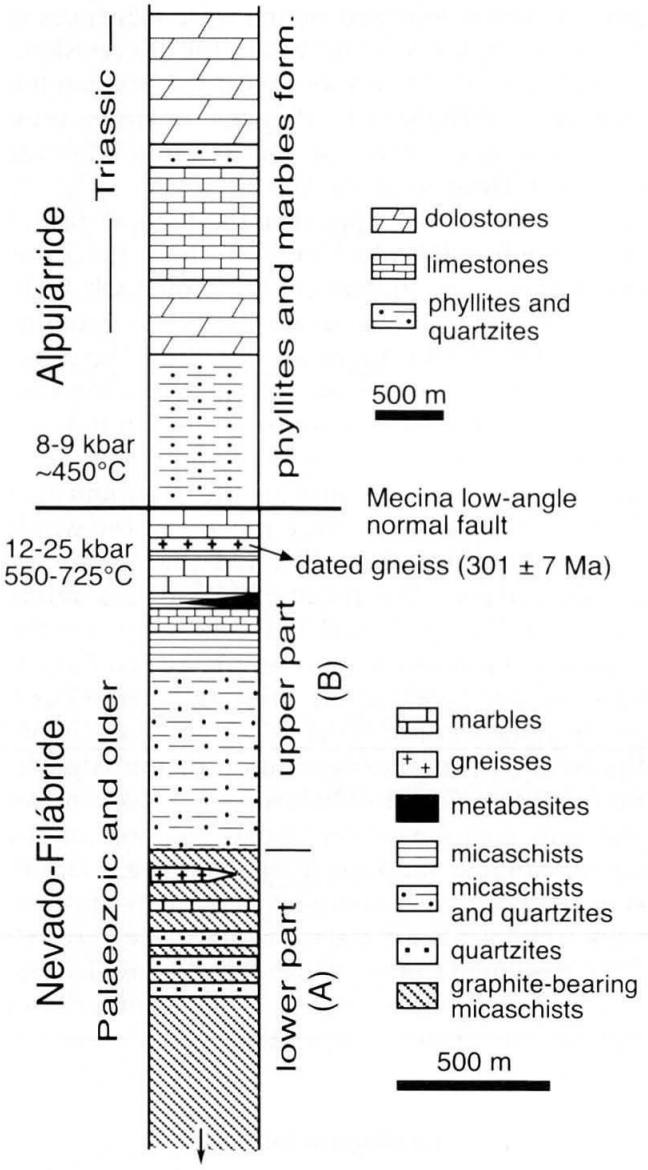

Fig. 2 Lithological succession observed in western Sierra Nevada. The Mecina low-angle normal fault separates the underlying Nevado-Filábride Complex from the overlying Permian-Triassic phyllites and Triassic marbles, traditionally attributed to the Alpujárride Complex. The lower arrow indicates that the thickness of the graphite-bearing metapelites is higher but unknown.

dred meters thick in the Sierra Nevada (B in Fig. 2). They consist of quartzites and micaschists followed by marbles and calcschists. Small (several meters) discontinuous bodies, dykes (millimeters to meters in size) and sheets (up to 5 meters thick) of mafic and acid igneous rocks occur within these upper metasediments and comprise small bodies of eclogites, amphibolites and gneisses. Ultramafic rocks form lenses of variable dimensions, up to hundreds of meters thick, most of them completely serpentinised.

The igneous and sedimentary rocks of the Nevado-Filábride Complex underwent Alpine metamorphism. Pressure-temperature (P–T) conditions of the early high-pressure event commonly range between 12 and 14 kbar and 550–600 °C (Gómez-Pugnaire and Fernández-Soler, 1987). Higher pressures and temperatures, however, have locally been determined (more than 18 kbar and 650–700 ° C, Gómez-Pugnaire et al., 1994; Trommsdorff et al., 1998; Puga et al., 2002). Later uplift produced a decompressional path that is not well constrained (Fig. 5). For most authors, decompression occurred with initial heating conditions followed by slight cooling in the amphibolite facies (Martínez-Martínez, 1986; Baker et al., 1989; Soto, 1993; Gómez-Pugnaire et al., 1994). Gómez-Pugnaire and Fernández-Soler (1987) proposed a slight heating during decompression before final cooling. Vissers (1981) described a similar path for high and intermediate pressures and a late reheating event at low pressures (2 kbar), analogous to Bakker et al. (1989) and De Jong (1991). Finally, Puga et al. (2000, 2002) are the only authors defining two consecutive Alpine metamorphic events (Eo-Alpine and Meso-Alpine) characterised by initial strong heating and compression, followed by rapid cooling and decompression.

The Nevado-Filábride Complex is overlain by phyllites, quartzites and carbonates, traditionally attributed to the lower units of the Alpujárride Complex (Fig. 2), which have been dated with fossils as Middle to Upper Triassic (Barrois and Offert, 1889; Martín and Braga, 1986; Braga and Martín, 1987). The phyllites immediately on top of the Nevado-Filábride Complex show high-pressure mineral assemblages formed at up to 9–10 kbar and 450–480 °C (Azañón and Goffé, 1997). The decompressional path of the phyllites is retrograde for most of the authors, but a late thermal overprint has been proposed by Bakker et al. (1989) and De Jong (1991).

The main contact separating the Nevado-Filábride and Alpujárride Complexes is, at present, a low-angle normal fault (the Mecina Fault), which was formed during exhumation, as were all of the ductile and brittle structures identifiable in the Nevado-Filábride Complex, and the brittle ones in the Alpujárride Complex. Most of the deformational structures of the Nevado-Filábride Complex were associated with the activity of the Alpujárride/Nevado-Filábride contact. For this reason, deformation gets more intense in the Nevado-Filábride Complex towards the contact with the Mecina Fault, which behaved as a ductile shear zone during the earlier stages of its development (Galindo-Zaldívar et al., 1989; Jabaloy et al., 1993). The sequence of structures that progressively formed in the Nevado-Filábride Complex, related to the extensional detachment that over-

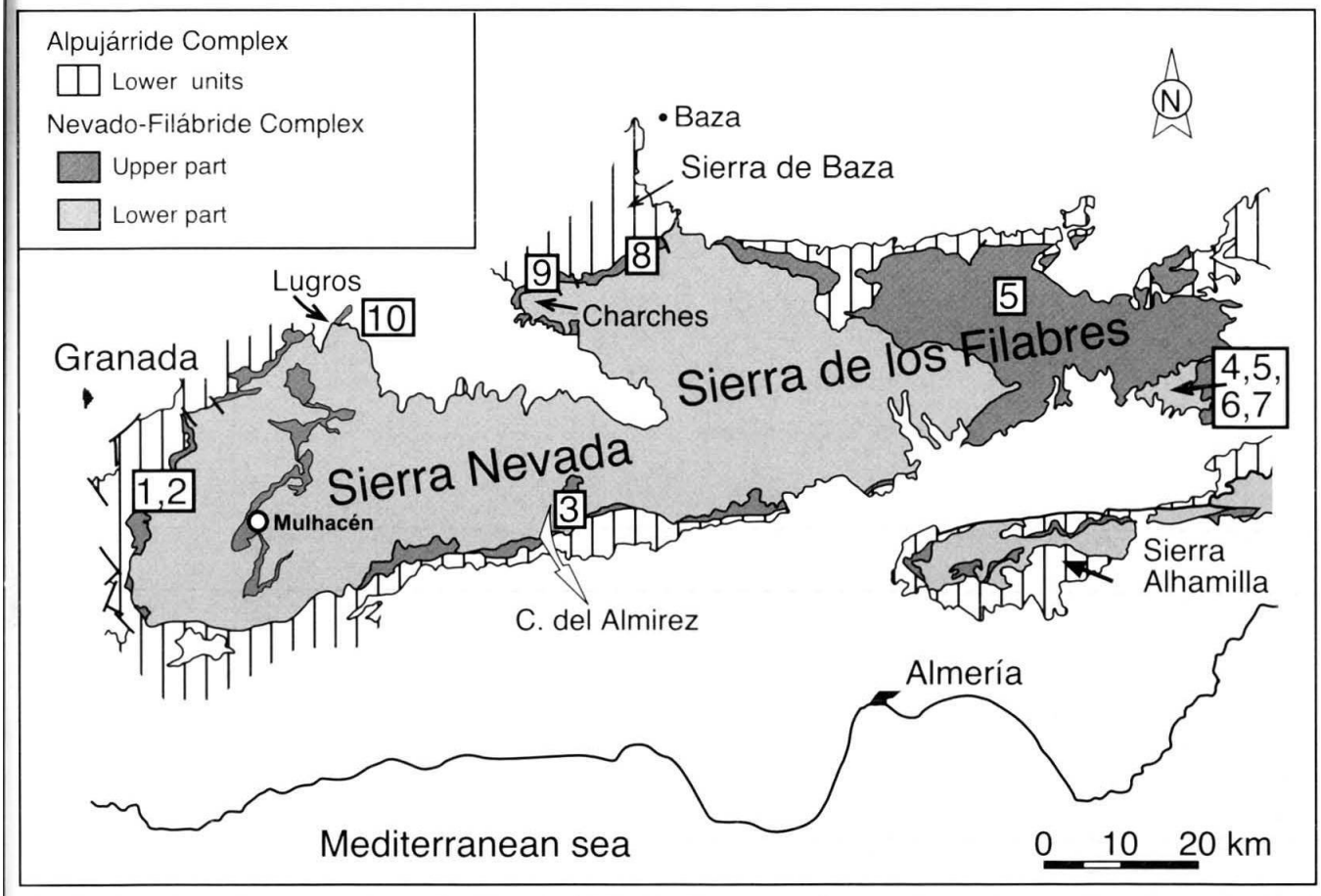

Fig. 3 Location of outcrops from the Nevado-Filábride Complex where radiometric ages have been obtained. 1: this paper; 2: Puga (1976); 3: López Sánchez-Vizcaíno et al. (2001); 4: Priem et al. (1966); 5: Andriessen et al. (1991); 6: Monié et al. (1991); 7: Nieto (1996); 8: De Jong (2003); 9: Gómez-Pugnaire et al. (2000); 10: Puga et al. (2003).

printed the sparse relics of previous penetrative structures, are as follows: (1) a low-dipping ductile foliation (the main foliation), axial planar to folds ranging in scale from microscopic to kilometric (Galindo-Zaldívar et al., 1988), and an associated stretching lineation, indicating the kinematic relationships at the Alpujárride/Nevado-Filábride contact in the early stages of its evolution (top-to-the W–SW); (2) overprinted ductile, ductile-brittle, and brittle extensional crenulation cleavages, more intense towards the top of the Nevado-Filábride Complex and locally forming two conjugate systems (Platt and Vissers, 1989; Jabaloy et al., 1993); (3) brittle deformation, represented by top-to-the W–SW low- and high-angle faults and joints, affecting the previous structures.

In the Alpujárride Complex the structures related to the extensional detachment are brittle. They overprint other ductile and ductile-brittle structures not related to the development of the Nevado-Filábride/Alpujárride contact as indicated by their older age (Monie et al., 1991, 23.5 ± 0.5 Ma, Fig. 3) and by their different kinematic relationships (Cuevas et al., 1986), which are characterised generally by ENE–WSW oriented stretching lineations, but with a top-to-the ENE sense of motion. These structural differences are consistent with a higher crustal position of the Alpujárride Complex since the onset of uplift (Galindo-Zaldívar et al., 1989).

Outcrop description

In this study we determined the age of one gneiss of the upper sequence of the Nevado-Filábride Complex at Collado de las Sabinas in the western Sierra Nevada, where gneisses outcrop close to the contact with the Alpujárride Complex (Fig. 1). The gneisses occur as sheets of variable thickness (centimeters to several meters), interlayered with marbles and light-coloured schists. The contact between gneisses and metasediments is sub-parallel to the main foliation, which dips gently westwards. All lithologies display a mylonitic foliation, a well-developed stretching and mineral lineation and, in some places, a prominent S-C fabric. Layered and *augen* structures in the gneisses can be found in the same outcrop. Fine-grained schists with alternating tourmaline-quartz-rich and gar-

Table 1 Representative microprobe analyses of minerals from: (A) gneisses, (B) light-coloured metapelites, (C) very-fine grained tourmaline-rich metapelites, (D) skarn-like rocks. (*) Analysis used in thermobarometric calculations.

Rock Type	(A)	(A)	(B)	(B)	(B)	(C)	(C)	(D)	(D)
	GARNET								
Description			core	core	rim *	core	rim	core	rim *
SiO_2	37.63	37.84	37.15	36.72	37.09	36.58	36.26	36.33	37.25
TiO_2	0.12	0.20	0.12	0.15	0.12	0.10	0.10	0.13	0.10
Al_2O_3	21.10	20.89	20.91	21.24	21.11	21.05	21.28	20.98	21.63
Cr_2O_3	0.02	0.02	0.00	0.00	0.00	0.02	0.00	0.03	0.03
Fe_2O_3	0.00	0.00	0.90	1.20	0.37	0.66	1.48	2.07	0.71
FeO	22.39	19.96	31.98	35.96	32.26	30.67	31.25	30.62	25.63
MnO	2.30	2.92	0.81	0.07	0.46	1.77	0.11	0.07	0.32
MgO	0.19	0.15	0.88	2.60	2.22	1.46	2.34	1.13	1.65
CaO	16.33	18.00	7.89	2.54	5.95	6.78	6.10	8.36	12.22
Total	100.09	99.99	100.65	100.50	99.59	99.03	98.78	99.73	99.54
formula: 16 cations and 24 oxygens									
Si	2.986	2.995	5.957	5.902	5.966	5.936	5.872	5.867	5.920
Ti	0.007	0.012	0.015	0.018	0.015	0.012	0.012	0.015	0.011
Al	1.973	1.949	3.953	4.025	4.004	4.027	4.062	3.995	4.053
Cr	0.001	0.001	0.000	0.000	0.000	0.001	0.000	0.002	0.002
Fe^{3+}	0.000	0.000	0.106	0.141	0.045	0.079	0.173	0.238	0.083
Fe^{2+}	1.486	1.321	4.185	4.697	4.295	4.085	4.066	3.912	3.325
Mn	0.154	0.196	0.110	0.010	0.062	0.243	0.015	0.009	0.043
Mg	0.023	0.018	0.211	0.622	0.533	0.354	0.564	0.273	0.392
Ca	1.389	1.526	1.356	0.437	1.026	1.179	1.059	1.447	2.081
Alm	0.49	0.43	0.71	0.81	0.73	0.70	0.71	0.69	0.57
Prp	0.01	0.01	0.04	0.11	0.09	0.06	0.10	0.05	0.07
Grs	0.46	0.50	0.23	0.08	0.17	0.20	0.19	0.26	0.36
Sps	0.05	0.06	0.02	0.00	0.01	0.04	0.00	0.00	0.01

Rock Type	(D)
	EPIDOTE
	*
SiO_2	37.58
TiO_2	0.15
Al_2O_3	26.43
Cr_2O_3	0.01
FeO_{tot}	8.61
MnO	0.09
MgO	0.03
CaO	23.16
Total	96.08
formula: O=12.5	
Si	2.977
Ti	0.009
Al	2.469
Cr	0.001
Fe^{3+}	0.565
Fe^{2+}	-
Mn	0.006
Mg	0.004
Ca	1.966
Pist	0.19
Ep	0.81

Rock Type	(A)	(A)	(B)	(B)	(B)	(C)	(C)	(D)	(B)
	WHITE MICA							BIO	
			small	big	*			*	*
SiO_2	48.28	48.68	48.72	48.79	48.01	46.33	47.05	47.97	37.59
TiO_2	0.38	0.39	0.62	0.46	0.55	0.37	0.35	0.24	1.52
Al_2O_3	29.30	28.33	32.90	31.71	32.30	34.53	33.89	33.98	17.53
Cr_2O_3	0.02	0.01	0.03	0.02	0.01	0.00	0.00	0.01	0.03
FeOt	4.95	5.39	1.60	1.63	1.27	1.43	1.30	2.67	18.51
MnO	0.04	0.01	0.00	0.00	0.01	0.00	0.02	0.01	0.03
MgO	1.44	1.52	1.47	1.63	0.43	0.84	0.95	0.89	11.93
CaO	0.01	0.01	0.01	0.01	1.57	0.08	0.01	0.04	0.17
Na_2O	0.12	0.12	1.47	1.20	1.43	1.45	1.41	0.77	0.23
K_2O	10.14	10.25	9.08	9.52	9.16	8.99	9.18	10.17	8.08
F	0.48	0.48	0.18	0.22	0.28	0.19	0.00	0.21	0.96
Cl	0.02	0.03	0.01	0.00	0.00	0.01	0.00	0.02	0.06
Total	95.18	95.26	96.09	95.19	95.01	94.22	94.16	96.98	96.64
O=F,Cl	0.21	0.21	0.08	0.09	0.12	0.08	0.00	0.09	0.09
∑cats-Ca-Na-K=6;O=11									formula: cats=13,O=23
Si	3.238	3.275	3.193	3.241	3.265	3.096	3.144	3.135	2.834
AlIV	0.762	0.725	0.807	0.759	0.735	0.904	0.856	0.865	1.166
AlVI	1.556	1.522	1.736	1.724	1.855	1.818	1.814	1.754	0.392
Ti	0.019	0.020	0.030	0.023	0.028	0.019	0.018	0.012	0.086
Cr	0.001	0.001	0.002	0.001	0.000	0.000	0.000	0.001	0.002
Fe^{3+}	–	–	–	–	–	–	–	–	–
Fe^{2+}	0.278	0.304	0.088	0.091	0.072	0.080	0.073	0.146	1.154
Mn	0.002	0.001	0.000	0.000	0.001	0.000	0.001	0.001	0.002
Mg	0.144	0.153	0.144	0.161	0.044	0.084	0.095	0.087	1.340
Ca	0.001	0.001	0.001	0.000	0.114	0.006	0.001	0.003	0.014
Na	0.015	0.015	0.187	0.155	0.189	0.187	0.183	0.098	0.033
K	0.867	0.880	0.759	0.806	0.881	0.767	0.782	0.848	0.777
F	0.154	0.153	0.056	0.071	0.086	0.061	0.000	0.065	0.338
Cl	0.003	0.005	0.001	0.000	0.000	0.001	0.000	0.003	0.011

Rock Type	(D)	(D)	(D)
	AMPHIBOLE		
	core	rim	rim *
SiO_2	44.29	39.29	36.27
TiO_2	0.40	0.25	0.08
Al_2O_3	14.98	16.65	18.49
Cr_2O_3	0.04	0.03	0.01
FeOt	14.44	22.94	23.77
MnO	0.01	0.13	0.09
MgO	7.35	3.38	2.55
CaO	8.98	10.65	10.68
Na_2O	2.86	2.11	2.14
K_2O	0.46	0.75	0.99
F	0.51	0.40	0.34
Cl	0.01	0.85	1.27
Total	94.32	97.71	96.68
O=F,Cl	0.22	0.55	0.71
formula: cats=13,O=23			
Si	6.745	6.119	5.757
AlIV	1.255	1.881	2.243
AlVI	1.434	1.176	1.217
Ti	0.005	0.003	0.010
Cr	0.045	0.029	0.002
Fe^{3+}	0.000	0.301	0.513
Fe^{2+}	1.840	2.687	2.643
Mn	0.001	0.018	0.013
Mg	1.668	0.784	0.603
Ca	1.465	1.777	1.817
Na	0.844	0.638	0.657
K	0.089	0.150	0.201
F	0.247	0.198	0.169
Cl	0.003	0.223	0.339

formula botite: ∑cats-Ca-Na-K=7, O=11

net–quartz–mica layers also occur overlying the gneisses and interlayered with them. Decimetric skarn-like lenses are found along the contact between the gneiss and light-coloured schists. They are brown massive rocks consisting of epidote + amphibole + garnet + quartz. Lens-shaped nodules, ranging in size from several millimetres to 25–30 cm, consisting of tourmaline + quartz, are common in the schists and scarcer in the gneisses. The adjacent lithologies and field relationships of the gneiss bodies at Collado de las Sabinas are similar to those of the gneiss layers dated by Gómez-Pugnaire et al. (2000) in Sierra de los Filabres, 50 km to the northeast (Fig. 3).

Similar gneisses are also found in the upper part of the underlying graphite-bearing schists (Fig. 2). They occur as centimetre to meter thick layers intercalated with dark metapelites. This suggests that a common magmatic episode affected the entire Nevado-Filábride sedimentary sequence.

There is general agreement about the igneous derivation of the protoliths of the gneisses. However, whether they are volcanic layers or tectonically flattened plutonic bodies is difficult to assert because of intense mylonitisation (Puga, 1976; Torres-Ruíz et al., 2003). The protoliths of discontinuous lenses of skarn-like rocks and of replacement tourmalinites, extending from several centimeters up to ten meters and up to one meter in thickness, are likely related to the emplacement of the igneous body.

Petrography

Gneisses

The studied gneisses are strongly deformed acidic igneous rocks, of probable plutonic origin, with a well-developed layered structure produced by metamorphic segregation. Mylonitic fabrics such as platy quartz, K-feldspar porphyroclasts, mica fishes and S-C-structures are common. Layers of recrystallised K-feldspar, quartz, tourmaline, minor plagioclase, titanite and epidote are intercalated with layers rich in muscovite, biotite, epidote and rutile and minor quartz and tourmaline. Accessory minerals, such as zircon and apatite, are usually included in tourmaline and micas. Fe-oxides are found in both types of layers. Angular and fragmented porphyroclasts (up to 4–5 cm long) of igneous K-feldspar are randomly distributed, displaying a conspicuous *augen* structure. White mica is a major component of the gneisses. It appears as small oriented crystals in the matrix and as elongated fishes parallel to the main foliation.

Tourmaline occurs as isolated crystals, frequently fractured, and up to several millimeters long. These usually display strong igneous zonation with thin, metamorphic, homogeneous overgrowths. Lens-shaped polycrystalline aggregates of tourmaline (several centimeters long) are also common.

Tourmaline-rich metapelites

They are fine to very–fine grained micaschists (average grain size up to 1 mm) consisting of alternating layers of tourmaline (up to 60%) + quartz, garnet (up to 50%) + quartz, and colourless mica + quartz + scarce biotite flakes + chlorite + allanitic epidote + rutile + Fe-oxides ± chloritoid.

Tourmaline is found in two textural occurrences:

1. Very small tourmaline crystals (0.02–0.05 mm) concentrated in layers of variable thickness (from millimetres to several decimetres), associated with quartz and minor white mica. The relative abundance and thickness of these tourmaline layers in the schists increase progressively towards the contact with the gneiss.

2. Folded and fragmented polycrystalline aggregates of quartz and tourmaline identical to those observed in the adjacent gneisses.

Garnet is concentrated in quartz-rich layers. It appears as very small (<0.02 mm) euhedral to subhedral crystals with dark cores due to abundant small inclusions.

Other metapelitic rocks

Light-coloured metapelites occur below and interlayered with the gneisses. Their mineralogical composition consists mainly of quartz and white mica, displaying compositional layering and garnet porphyroblasts (up to 2 mm). Euhedral tourmaline crystals (up to 3 mm long) are unusually abundant in these metapelites at the contact with the gneiss, in comparison to similar light-coloured schists away from the gneiss body. Biotite, rutile, ilmenite, clinozoisite-rich epidote and zircon appear as accessory minerals.

White mica in metapelites occurs as strongly recrystallised grains in the form of sheared porphyroblasts or as crystals with a mimetic preferred orientation parallel to the foliation. Garnet crystals show two texturally and compositionally different zones (Fig. 4): a core with abundant quartz, tourmaline, and rutile inclusions, locally displaying rotational patterns, and an inclusion-free, euhedral overgrowth.

Tourmaline occurs as isolated euhedral crystals or as aggregates with textures and chemical com-

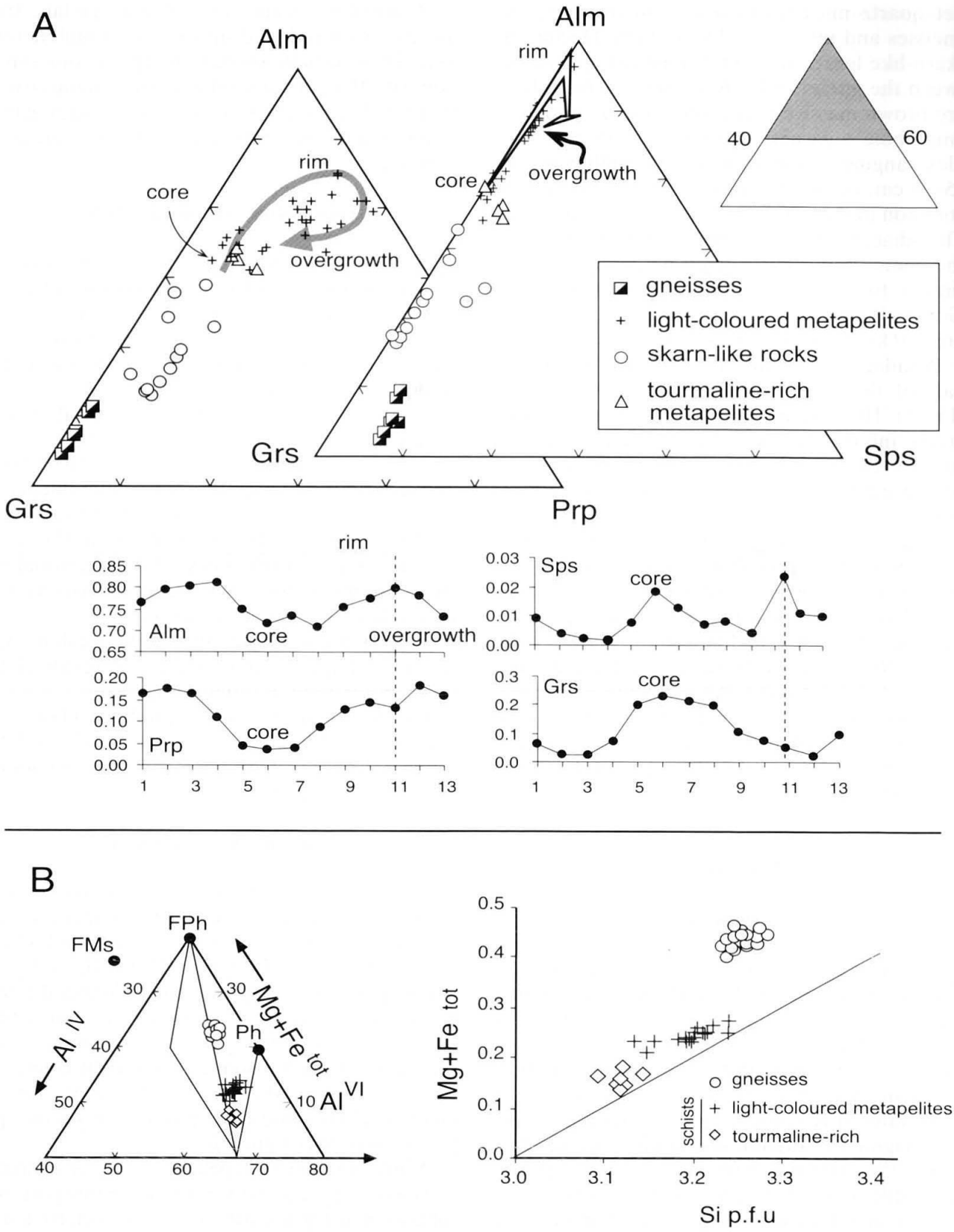

Fig. 4 Compositional variations of garnet (A) and white mica (B) from all rock types.

position similar to those described in the gneisses and tourmaline-rich metapelites by Torres-Ruiz et al. (2003). Clinozoisite-rich epidote (70–75 mol%) and rutile are the most common accessory minerals. Rutile shows ilmenite rims, except where it appears as inclusions in garnet cores.

Two generations of minerals can be distinguished according to textural relationships. The

first one comprises the garnet cores, the large colourless mica flakes, rutile and zoisite/clinozoisite, while the second generation consists of the garnet overgrowth, colourless mica in the foliated matrix and the ilmenite rims around rutile. Metamorphic recrystallisation of tourmaline possibly took place in both generations.

Skarn-like rocks

They are strongly mylonitised rocks showing a uniform mineralogical composition. They consist of amphibole, epidote, garnet and quartz as essential minerals with rutile, titanite, Fe-oxides and zircon as accessory ones.

The geological setting of this type of gneiss is very similar throughout the upper part of the Nevado-Filábride Complex. Although deformation in gneisses and in host metasediments is intense, there are several lines of evidence pointing to an intrusive origin of contacts between igneous bodies and metasediments, rather than a late tectonic emplacement:

(a) The abundance of tourmaline in gneisses and adjacent rocks. This mineral may occur as: (i) abundant veins and lenses cutting across gneisses and micaschists or intercalated with them; (ii) replacement tourmalinites in the metasediments, (iii) the unusually high tourmaline modal content in metapelites adjacent to the gneisses. Tourmaline concentrations found in both the gneisses and adjacent metapelites have been interpreted as the result of post-magmatic hydrothermal processes related to the exsolution of B-rich fluids released from the meta-felsic igneous rocks (Voet, 1967; Torres-Ruiz et al., 2003).

(b) The occurrence of skarn-like rocks at the gneiss-metapelite interface formed by hydrothermal transfer between the intruded granitic bodies and the sedimentary wall rocks (Nieto, 1996). The present mineral assemblages observed in these rocks, however, are related to recrystallisation during regional metamorphism (Helmers, 1982).

Mineral composition

Table 1 shows compositional variations of minerals in all lithologies and the analyses from metapelite and amphibole–epidote-rich samples used in the thermobarometric calculations. Samples were analysed by electron microprobe Cameca SX50 at the Universidad de Granada. An acceleration voltage of 15 kV, a beam current of 20 nA, and a beam diameter of 8 μm were used. Standards were natural and synthetic compounds. Data were reduced using the PAP procedure of Pouchou and Pichoir (1985).

Garnet in gneisses appears as rounded or subhedral crystals with a restricted compositional range: Alm_{42-49}, $Sps_{5-6.5}$, $Prp_{0.6-0.9}$, Grs_{45-51} either from core to rim or among different crystals or samples (Fig. 4). This garnet composition, rich in grossular and almandine end members, is comparable to that previously reported for the same rocks (Nieto, 1996; Torres-Ruiz et al., 2003). Garnet in metapelites is richer in almandine and lower in spessartine contents. Zoning from cores to interfaces with overgrowths is characterised by increasing almandine and pyrope and decreasing grossularite contents (Fig. 4). An inverse pattern, especially for the almandine end-member, is observed in overgrowths. Garnet cores are compositionally very similar to garnet in tourmaline-rich metapelites, which are very homogeneous at the scale of single grains and thin section (Fig. 4).

White micas have a very restricted compositional variation in the gneisses irrespective of their textural sites. They are phengitic with paragonite contents <7 mol%. In metapelites phengite has paragonite contents of up to 20 mol% and lower Fe contents. Phengitic muscovite has even lower Fe and Si contents in tourmaline-rich metapelites. The chemical variation of white micas is essentially related to the different bulk composition of the samples. Nevertheless, micas in metapelites show a clear variation in (Fe+Mg) versus Si and Al^{tot} contents (Tschermak substitution) that may account for different metamorphic conditions (Fig. 4).

Clinozoisite-rich (up to 95 mol%) epidote is common in the gneisses both as very-fine grained aggregates and as isolated crystals associated with tourmaline. Allanite occurs in the core of clinozoisite crystals within aggregates. Titanite is a frequent accessory in leucocratic layers, occurring as anhedral to subhedral very fine-grained crystals, with relatively high Al contents (0.235 p.f.u.), which show a positive correlation with F (0.118 p.f.u.) (Torres-Ruiz et al., 2003). In skarn-like samples, orthozoisite (up to 90 mol%) partially altered to pistacitic epidote (up to 54 mol%) constitutes up to 40 mol%. Amphibole cores are ferro-pargasite, rims are ferro-hornblende. Garnet displays rounded and euhedral overgrowths partially replaced by amphibole. Their chemical composition is intermediate between garnet in the gneisses and in metapelites (Fig. 4).

Metamorphic evolution

The upper part of the Nevado-Filábride Complex underwent high-pressure metamorphism (Fig. 5) at maximum P and T conditions between 18–25

kbar and 625–725 °C (Gómez-Pugnaire et al., 1994; López Sánchez-Vizcaíno et al., 2001; Puga et al., 2002). In the studied gneisses and adjacent metapelites and skarns, we tried to estimate the conditions of formation of the mineral assemblages interpreted to have equilibrated during the peak of metamorphism. We used the program THERMOCALC v3.21 and the thermodynamic dataset of Holland and Powell (1998, modified 1999) to apply the average P–T method of Powell and Holland (1994). The high thermodynamic variance of the stable mineral assemblages in the gneiss precludes any direct estimation of their metamorphic evolution. In this kind of rocks high-pressure assemblages are not preserved due to intense low temperature retrograde overprinting, strongly favoured by hydration reactions during exhumation (Heinrich, 1982; Proyer, 2003). However, relics of high-pressure assemblages have been described in the metagranites and orthogneisses from other parts of the Nevado-Filábride Complex (Nieto, 1996; Nieto et al., 1997). These authors estimated metamorphic conditions for the high-pressure climax ranging from 12–14 kbar and 500–600 °C in the eastern part of the complex to 18–22 kbar and 650–700 °C in the western part (Fig. 5).

In contrast, significant constraints on the metamorphic evolution (Fig. 5) were derived from fine-grained metapelites and skarn-like rocks interlayered with the gneisses. In zoned minerals, only rim compositions were used for the calculations, as

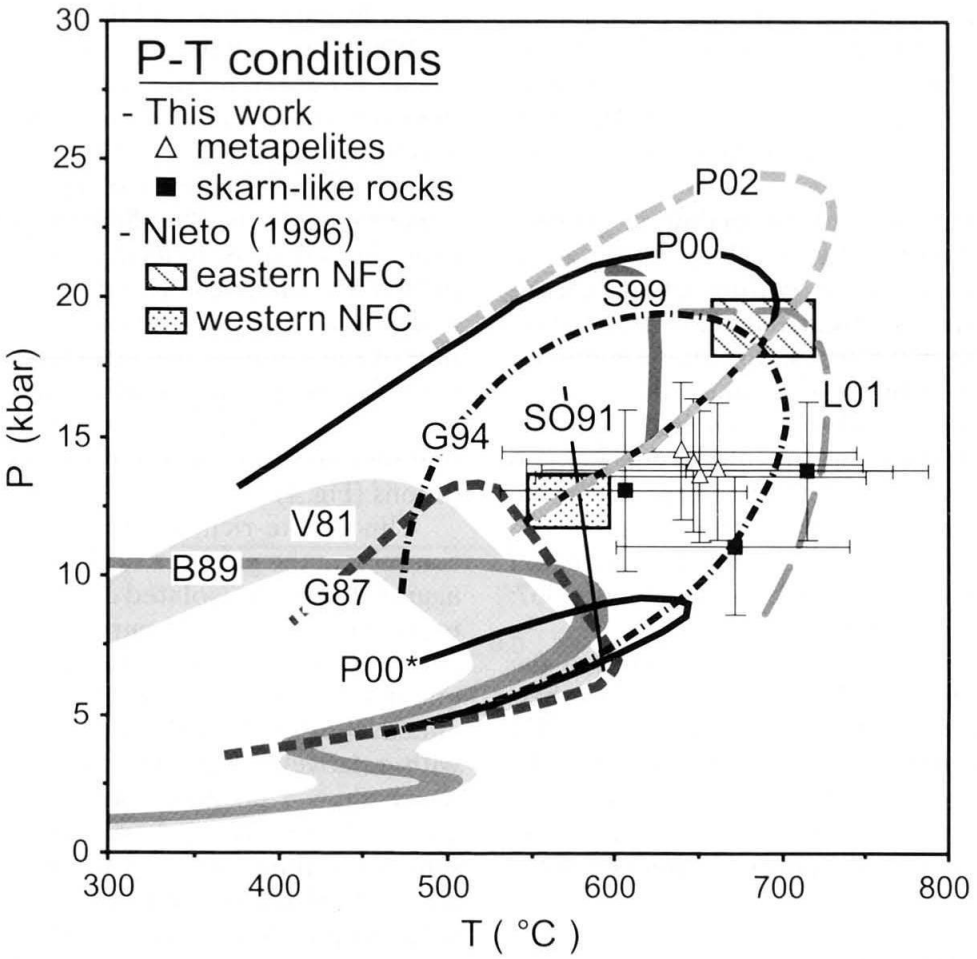

Fig. 5 P–T conditions deduced from metapelites (triangles) and skarn-like samples (squares) that alternate with the dated gneiss from Collado de las Sabinas (Sierra Nevada, SN). Error bars represent one standard deviation from the average P–T values shown in Table 2. Thermobarometric estimations by Nieto (1996) made on metagranites and gneisses from outcrops in the eastern (box with stripes) and western (box with dots) Nevado-Filábride Complex are shown for comparison. P–T paths from different areas and rock types of the Nevado-Filábride Complex are also shown. V81—(Vissers, 1981): metapelites of the central Sierra de los Filabres (SF); G87—(Gómez-Pugnaire and Fernández Soler, 1987): metabasites of the Sierra de Baza; B89—(Bakker et al., 1989): metapelites and metabasites of the eastern SF; SO91—(Soto, 1991): metapelites of the eastern SF; G94—(Gómez Pugnaire et al., 1994): metaevaporites of the eastern SF; S99—(Schönbächler, 1999): metapelites of the Cerro del Almirez (central SN); P00—(Puga et al., 2000): metabasites of the eastern SN—(their Eo-Alpine metamorphic event); P00*—(Puga et al., 2000): metabasites of the eastern SN (their Meso-Alpine metamorphic event); L01—(López Sánchez-Vizcaíno et al., 2001): ultramafic rocks of the Cerro del Almirez (central SN); P02—(Puga et al., 2002): ultramafic rocks of the Cerro del Almirez.

they most probably reflect peak metamorphic conditions. P–T conditions obtained for these two lithologies are shown in Table 2. For metapelites, P–T conditions were calculated using equilibria between garnet, muscovite, epidote, biotite, and quartz (Table 1). Results obtained range from 640 ± 106 to 662 ± 106 °C and 13.8 ± 2.5 to 14.5 ± 2.5 kbar (Table 2, Fig. 5). P–T estimates obtained for garnet and muscovite pairs are not precise enough to constrain metamorphic conditions. In the case of skarn-like rocks, P–T estimates obtained for the assemblage garnet, white mica, green amphibole, epidote, and quartz (Table 1) range from 605 ± 74 to 715 ± 72 °C and 13.0 ± 2.9 to 13.7 ± 2.5 kbar (see Table 2, Fig. 5).

The obtained results plot in a PT diagram (Fig. 5) at intermediate conditions between those reported by Nieto (1996) for the gneisses from the eastern part of the Nevado-Filábride Complex and those of the western part. Estimated temperatures, especially those of skarns, are close to the highest values ever estimated in any Nevado-Filábride rock. Pressures, however, are significantly lower than peak pressure values reported for different rock types of this complex (Fig. 5). Despite this, the metamorphic conditions calculated here for the wall rocks of the dated gneiss are taken to confirm that the Nevado-Filábride gneisses underwent the same metamorphic evolution that the rest of the complex, including high pressure conditions (P > 11 kbar).

Geochronology

Methods

Zircon was prepared as mineral separates from the augen gneiss mounted in epoxy and polished down to expose the grain centres. Cathodoluminescence investigation of zircon was carried out at the Electron Microscope Unit, Australian Nation-

Table 2 Thermobarometric data for skarns and metapelites.

Pelite assemblage: sample SAB 3-4
Independent set of reactions and calculations (for T = 530 °C and X_{H2O} = 1.0)

	P(T)	sd(P)
1) mu + 2phl + 6q = py + 3cel	14.7	2.68
2) 2east + 6q = py + mu + cel	10.2	2.90
3) 5py + 15cel + 12cz = 8gr + 15east + 57q + $6H_2O$	9.5	2.94
4) py + ann = alm + phl	16.9	22.55

T = 648 °C, sd = 101 °C; P = 14.0 kbar, sd = 2.4 kbar, cor = 0.208, sigfit = 1.27

Results for other samples:
SAB 3-3: 662 ± 106 °C and 13.8 ± 2.5 kbar
SAB 3-5: 652 ± 99 °C and 13.6 ± 2.4 kbar
SAB 3-6: 640 ± 106 °C and 14.5 ± 2.5 kbar

Skarn assemblage: SAB 2-6
Independent set of reactions and calculations (for T = 530 °C and X_{H2O} = 1.0)

	P(T)	sd(P)
1) 9ts + 4gr + 6q = 3tr + 12cz + 4py	15.9	6.93
2) 19ts = 3tr + 16cz + 14py + $8H_2O$	18.7	5.92
3) 78fact + 105ts = 63tr + 80gr + 130alm + 120q + $120H_2O$	11.7	4.12
4) ts + 2cel = tr + 2mu	10.0	25.16
5) 57ts + 6gl + 28gr = 15tr + 12parg + 72cz + 22py	15.7	9.15
6) 19tr + 4parg + 24cz + 26py + 28pa = 47ts + 16gl	19.6	9.25

T = 715 °C, sd = 72 °C, P = 13.7 kbar, sd = 2.5 kbar, cor = 0.264, sigfit = 1.28

Results for other samples:
SAB 2-2: 671 ± 70 °C and 11.0± 2.5 kbar
SAB 2-4: 605 ± 74 °C and 13.0 ± 2.9 kbar

sd: standard deviation. 1σ uncertainty
cor: PT correlation coefficient (Powell and Holland, 1994)
sigfit: measure of the scatter in residuals of the enthalpies and activities normalized by their uncertainties

al University, with a HITACHI S2250-N scanning electron microscope working at 15 kV, ~60 nA, and ~20 mm working distance.

Trace element analyses were performed by Laser Ablation-ICP-MS at the Research School of Earth Sciences (RSES) using a pulsed 193 nm ArF Excimer laser with 100 mJ energy at a repetition rate of 5 Hz, coupled to an Agilent 7500 quadrupole ICP-MS (Eggins et al., 1998). Laser sampling was performed in a He atmosphere using 54 μm spot diameter for zircon cores and 19 μm for metamorphic rims. Data acquisition was performed by peak hopping in pulse counting mode, acquiring individual intensity data for each element during each mass spectrometer sweep. During the time-resolved analysis, contamination from inclusions, fractures and zones of different composition was detected by monitoring several elements. A synthetic glass (NIST 612) was used as standard material. Internal standard was stoichiometric Si. Oxides, which are often a source of interference, were reduced to a minimum (ThO/Th < 0.4%) by ICP-MS tuning.

U–Th–Pb analyses were performed using a sensitive, high-resolution ion microprobe (SHRIMP II). Instrumental conditions and data acquisition were generally as described by Compston et al. (1992). The data were collected in sets of six or seven scans throughout the masses. The measured $^{206}Pb/^{238}U$ ratio was corrected using reference zircon from a gabbro of the Duluth Complex in Minnesota (AS3, 1099 Ma, Paces and Miller, 1993), whereas a zircon of known composition (SL 13) was used to determine the U content of the target. The data were corrected for common Pb on the basis of the measured $^{208}Pb/^{206}Pb$, as described by Compston et al. (1992). The composition of the common Pb has been assumed to be that of Broken Hill Pb ($^{204}Pb/^{206}Pb$ = 0.06250, $^{207}Pb/^{206}Pb$ = 0.96180 and $^{208}Pb/^{206}Pb$ = 2.22850), which is known to be common Pb instrumental background. Age calculations were done using the software Isoplot/Ex (Ludwig 2000). Isotopic ratios and single ages are reported with 1σ errors, whereas mean ages are at 95% confidence level.

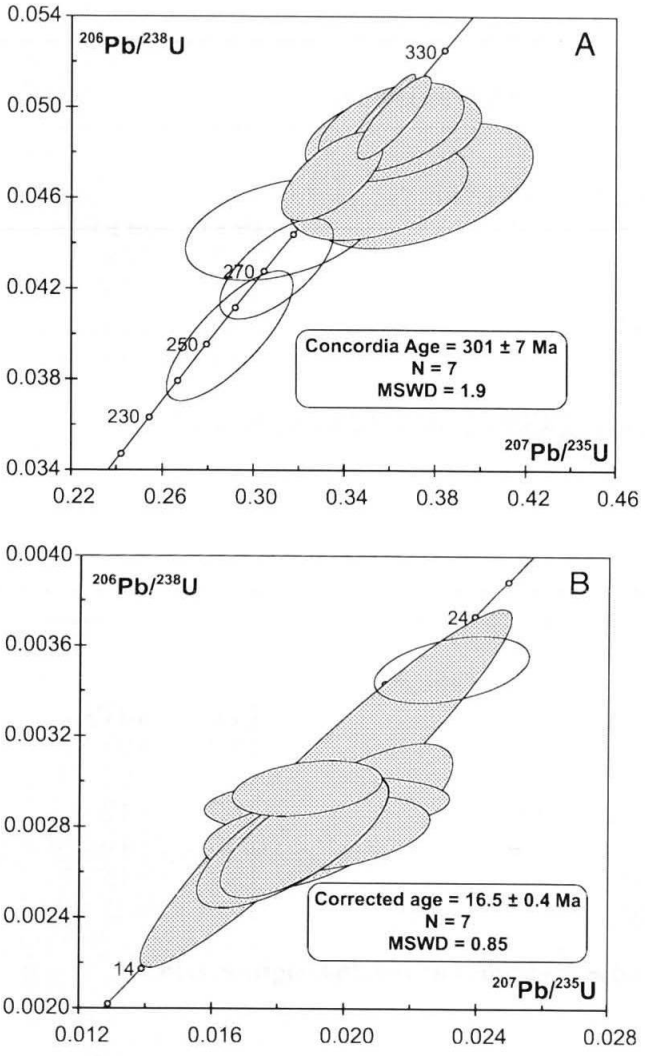

Fig. 6 Concordia diagram for SHRIMP analyses. Unfilled symbols represent data excluded from the age calculation. In (A), the mean age has been corrected for the matrix effect caused by the high U content of the zircon. See text for explanation. Mean ages are at 95% c.l.

Zircon description

Zircon crystals recovered from sample S00 are mainly euhedral and milky to colourless. Most zircon grains display fine oscillatory zoning parallel to the crystal faces (Fig. 7A, C and D) as generally observed in zircon from granitic rocks. Some crystals have a complex structure with concentric domains that suggest more than one magmatic growth stage. In a small number of crystals, the magmatic zircon shows embayments which crosscut the magmatic oscillatory zoning and are filled with dark, apparently homogeneous zircon.

Of the total zircon crystals, 20 to 30% do not have oscillatory zoning, but a fine, mosaic-like zoning pattern with dark CL emission (Fig. 7C). In a few grains, the mosaic-like texture is overgrown by oscillatory-zoned zircon.

Inclusions are found in a number of crystals, particularly in those with a mosaic-like zoning pattern. In most cases the included mineral are quartz and albite, with minor epidote. A titanite inclusion was found in one unzoned rim.

U–Pb dating

SHRIMP U–Pb analyses were performed on oscillatory-zoned domains and the dark, unzoned

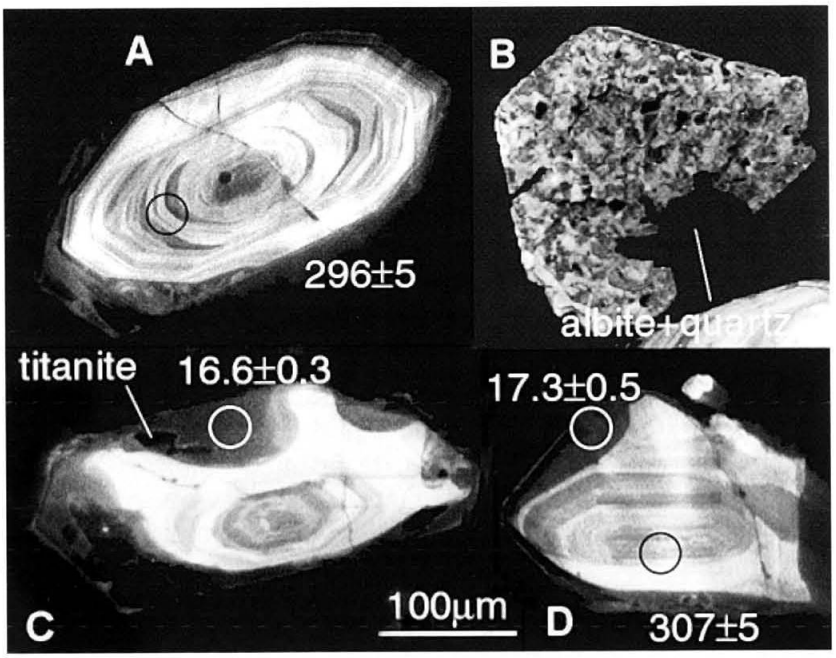

Fig. 7 Cathodoluminescence images of zircon crystals from the dated gneiss. Crystals A, C and D consist of core parts with magmatic oscillatory zoning, each overgrown by a dark, unzoned rim yielding a metamorphic age. Note the inclusion of titanite in crystal C. Crystal B is from the same sample, but has a mosaic-like zoning pattern, which is often indicative of perturbation of the U–Pb system. Scale bar refers to all crystals.

overgrowths. The mosaic-like crystals were not analysed because this zoning has been previously associated with alteration and lead loss (Pidgeon et al., 1998; Rubatto et al., 1998; Rubatto and Hermann, 2003) and thus such crystals were likely to yield geologically meaningless ages. Ten analyses on the oscillatory domains yielded apparent $^{206}Pb/^{238}U$ ages between 253 ± 7 and 312 ± 5 Ma (Table 3). Seven analyses form a cluster on concordia with an age of 301 ± 7 Ma (Fig. 6), which is interpreted as dating the formation of the zircon. The other three analyses yield younger ages (Table 3). These younger values correspond to zircon domains that could have easily been affected by Pb loss during metamorphism and fracturing. In fact, one analysis corresponds to a zircon core, which is overgrown by a younger unzoned rim; a second one was measured close to the border of the crystal; and the third one was performed close to a fracture.

The unzoned rims yield much younger ages than the oscillatory-zoned domains. Seven analyses out of eight form a tight cluster on concordia around 18 Ma (Fig. 6, Table 3). One analysis measured on a particularly small rim (~ 20 μm) is significantly older (22.5 ± 0.4 Ma) probably because the SHRIMP spot partly overlapped the older core. The analysed rims have extremely high U contents (up to 5500 ppm), a composition that could produce a matrix effect and an apparent increase in $^{206}Pb/^{238}U$ ages, as described in zircon with more than 2500 ppm of U (Butera et al., 2001). In fact, the $^{206}Pb/^{238}U$ age of the overgrowths dated at around 18 Ma shows positive correlation with U content (R = 95), with the exclusion of one analysis. This indicates that the ages obtained are likely to be too old because of the zircon composition and a correction has to be applied for compositions over 2500 ppm U (see Butera et al., 2001). The correlation between age and U-content indicates that the $^{206}Pb/^{238}U$ age increases 1.0074 Ma each 1000 ppm of U. After correction, the mean age of the seven younger analyses on unzoned zircon rims is 16.5 ± 0.4 Ma (MSWD = 0.85).

Zircon composition

The oscillatory-zoned domains and a few dark, unzoned overgrowths were analysed by LA-ICPMS (Table 4) for P, Ti, Sr, Y, Nb, REE, Hf, Th and U (these last two elements were also measured during SHRIMP analysis, see Table 3). The magmatic cores contain significant amounts of P, Y, REE, Hf, Th and U. Their chondrite-normalised patterns (Fig. 8) show a progressive enrichment from LREE to HREE with a positive Ce-anomaly and a strong negative Eu-anomaly. These features are known from magmatic zircon in granitic rocks (Hinton and Upton, 1991; Belousova et al., 2002; Whitehouse and Kamber, 2002). The enrichment in HREE is due to the zircon crystal structure and the fact that heavy REE are smaller in ionic radius and thus fit the Zr site better. Positive Ce-anomaly in zircon is attributed to

the presence of Ce^{+4}, which easily substitutes for Zr^{4+}. The negative Eu anomaly is due to the co-precipitation of feldspar, a Eu-rich phase ubiquitous in granitic rocks.

Only two analyses of zircon overgrowths were obtained due to their small dimensions (Table 4). They are distinguished from the oscillatory domains by their lower contents in many trace elements including P, Ti, Y, HREE, and Th. They are, however, richer in Nb and extremely rich in U. One of the analyses shows a strong enrichment in LREE and Sr, which is unusual for zircon and could be due to either micro-inclusions of fluid or to incorporation of LREE in radiation-damaged regions (Whitehouse and Kamber, 2002). The most remarkable feature of the zircon overgrowths is a REE pattern which, in contrast to the oscillatory domains, is flat in the HREE (Fig. 8).

Discussion

Age interpretation

The zircon domains dated at 301 ± 7 Ma have magmatic characteristics: oscillatory zoning, Th/U between 0.03 and 0.3, and a steep REE pattern enriched in HREE. The formation of these domains is interpreted as dating the crystallisation of the granitic protolith of the gneiss.

On the other hand, the 16.5 ± 0.4 Ma zircon overgrowths have metamorphic features: they crosscut the magmatic zoning, have no regular zoning pattern, and their Th/U is low (0.002–0.004). The low trace element contents of these overgrowths is another indication of formation in a metamorphic environment (Hoskin and Black, 2000; Rubatto, 2002), which is generally poorer in trace elements than a granitic melt. The high contents in Nb and U could be an indication that this zircon formed in a surrounding locally enriched in these elements and where no other phase could host them. The breakdown of rutile to form titanite during decompression could have supplied Nb, whereas the sources of U are uncertain (monazite, allanite or partial dissolution of magmatic zircon).

Establishing the conditions at which the metamorphic zircon overgrowths formed is difficult due to the lack of diagnostic mineral assemblages. The inclusions of quartz and albite found in the overgrowths are not particularly significant. Assuming that the titanite inclusion (Fig. 6C) is primary, i.e. was included in the zircon at the time of formation and not through later fractures, it indicates that the zircon did not form at the HP peak, where rutile would be stable. The flat REE pattern of the zircon overgrowths indicates that they formed in the presence of a mineral phase that sequestered the HREE. In other studies, this phase has been demonstrated to be garnet (Ru-

Table 3 U–Pb SHRIMP data of zircon. The age of metamorphic rims has been corrected for matrix effect due to high U content; see text for explanation.

Label	ppm U	ppm Th	Th/U	% Pb com	$^{207}Pb/^{235}U \pm 1\sigma$		$^{207}Pb/^{206}Pb \pm 1\sigma$		$^{206}Pb/^{238}U \pm 1\sigma$		Age $^{206}Pb/^{238}U \pm 1\sigma$		Corrected Age	
magmatic cores														
S00-2.2	3136	89	0.029	0.04	0.3615	67	0.0529	5	0.04959	74	312	5		
S00-3.4*	208	30	0.148	0.94	0.3116	172	0.0506	25	0.04469	91	282	6		
S00-4.2	487	131	0.277	0.09	0.3601	131	0.0531	16	0.04915	81	309	5		
S00-5.1	3753	124	0.034	0.03	0.3493	88	0.0520	4	0.04875	112	307	7		
S00-7.2	1010	38	0.039	0.13	0.3343	91	0.0516	10	0.04701	79	296	5		
S00-8.2	440	63	0.147	0.56	0.3548	160	0.0555	22	0.04633	86	292	5		
S00-10.1	777	252	0.335	0.24	0.3611	159	0.0537	21	0.04880	72	307	5		
S00-11.1*	819	51	0.064	0.33	0.3097	102	0.0523	26	0.04297	90	271	6		
S00-12.1	646	54	0.087	0.29	0.3742	198	0.0582	12	0.04662	112	294	7		
S00-13.1*	1957	84	0.045	0.65	0.2892	114	0.0524	0	0.04004	116	253	7		
metamorphic rims														
S00-3.1	4214	9	0.002	0.60	0.0188	10	0.0490	18	0.00277	11	17.9	0.7	16.1	0.7
S00-3.2	4127	12	0.003	0.48	0.0184	12	0.0486	20	0.00275	12	17.7	0.8	16.1	0.8
S00-3.3	5487	14	0.003	0.76	0.0189	9	0.0459	21	0.00298	5	19.2	0.3	16.2	0.3
S00-4.1	4774	15	0.003	0.39	0.0201	13	0.0509	21	0.00286	13	18.4	0.8	16.1	0.8
S00-6.1*	2818	10	0.004	0.88	0.0232	10	0.0481	18	0.00350	6	22.5	0.4	22.2	0.4
S00-8.1	5537	10	0.002	0.61	0.0194	23	0.0473	16	0.00298	32	19.2	2.1	16.1	2.1
S00-9.1	4656	12	0.003	1.92	0.0195	15	0.0484	36	0.00291	5	18.8	0.3	16.6	0.3
S00-10.2	3019	6	0.002	1.40	0.0191	14	0.0500	32	0.00278	7	17.9	0.5	17.3	0.5

*; excluded from the mean age calculation
Corrected age; age corrected for high U content in zircon (see text for details)

batto, 2002; Rubatto and Hermann, 2003; Whitehouse and Platt, 2003). Garnet was not observed in the sample dated, but it is present in adjacent layers of the same rock. The possibility that metamorphic zircon records the chemical signature of garnet present elsewhere (less than 15 cm away) in the rock is not unlikely, considering that metamorphism was possibly associated with fluid circulation (see high LREE in zircon rim). Other phases in the mineral assemblage capable of storing a significant amount of HREE are titanite, which was found as an inclusion in the zircon overgrowths, and allanite, which is a rare accessory. The inclusion of titanite in the zircon rim, together with the need for garnet, titanite or allanite as sink for HREE, would suggest that the metamorphic zircon overgrowths formed during decompression, when titanite and garnet were stable.

Geological implications of the age of the protolith

The age of 301 ± 7 Ma for the gneiss protolith has significant implications concerning the age of deposition of the upper part of the Nevado-Filábride Complex and the relative stratigraphic and tectonic evolutions of both the Alpujárride and the Nevado-Filábride Complexes.

The dated gneiss body occurs within the marbles and micaschists at the top of the lithostratigraphic succession of the Nevado-Filábride Complex. The SHRIMP data imply a Carboniferous or even older age for the marbles, which have been considered as Triassic; hence the complete sequence of the upper part of the complex must be Palaeozoic in age.

Younger Rb–Sr ages (215 ± 15 Ma) were obtained by Puga (1976) for gneisses of the same outcrop and by Gómez-Pugnaire et al. (2000; 247 ± 11 Ma) on equivalent gneiss bodies from the western Sierra de los Filabres (Fig. 3). The younger ages might be explained by the less robust dating method adopted by these authors when compared with U–Pb ion microprobe analysis on single zircon domains. Alternatively, these ages may reflect that the acid igneous activity took place over a long time span, a continued post-magmatic activity or even a metamorphic event related to the extensional tectonic associated with the Pangea break-up (Angles et al., 1999). In any case, the minimum deposition age of the metasediments of the upper part of the Nevado-Filábride complex would be that of the oldest dated igneous body, i.e. 301 ± 7 Ma.

The significance of the Alpujárride/Nevado-Filábride contact

The Nevado-Filábride Complex is always overlain by the dated (Barrois and Offert, 1889; Martín and Braga, 1986; Braga and Martín, 1987) Permo-Triassic phyllites and Triassic marbles of the lower Alpujárride units (Fig. 1). The evidence that high-pressure metamorphism affected both complexes indicates that they underwent a common evolution from the beginning of subduction. Further, the lower pressures and temperatures deduced for the Alpujárride Mesozoic rocks (Goffé et al., 1989; Azañón, 1991) indicate that these rocks were located in an upper crustal position with respect to the Nevado-Filábride Complex. The different regime of development of the extensional structures: ductile conditions in the Ne-

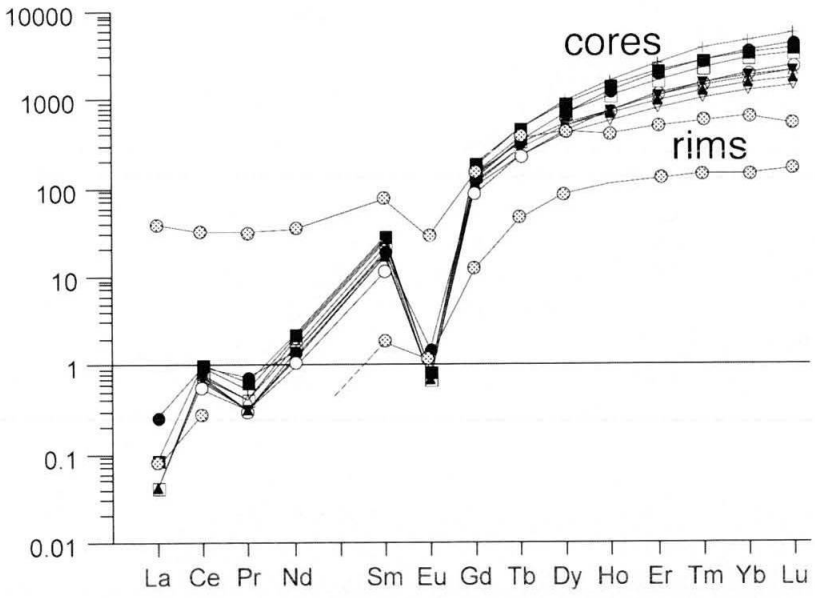

Fig. 8 Chondrite normalised pattern of zircon from the gneiss.

Table 4 Trace element composition of zircon cores and rims measured by LA-ICPMS.

	10 rim	09 rim	10 core	03 core	04 core	15 core	09 core	14 core	12 core	16 core
P	394	28	1061	1448	1724	1020	1101	835	1087	2002
Ti	2.42	bdl	4.68	9.23	8.43	5.54	6.35	5.75	6.39	10.86
Sr	2.28	0.20	0.32	0.78	1.07	0.27	0.29	0.25	0.31	0.54
Y	666	241	1225	1822	2335	1197	1259	945	1253	2705
Nb	2.21	2.02	0.51	0.74	0.94	0.69	0.56	0.53	0.61	0.76
La	9.01	0.02	bdl	0.01	0.02	0.01	0.01	0.00	0.00	0.00
Ce	20.26	0.17	0.32	0.46	0.64	0.39	0.48	0.43	0.44	0.59
Pr	3.05	bdl	0.03	0.04	0.06	0.03	0.04	0.03	0.03	0.05
Nd	16.59	bdl	0.44	0.74	1.07	0.57	0.92	0.56	0.66	0.99
Sm	11.18	0.28	1.69	3.24	4.48	2.52	3.75	2.54	2.84	4.01
Eu	1.66	0.07	bdl	0.04	0.05	0.04	0.05	0.04	0.04	0.05
Gd	29.3	2.6	17.9	27.3	38.6	22.4	29.0	21.5	25.1	36.3
Tb	13.10	1.69	8.20	12.59	17.31	10.09	11.57	8.71	10.50	17.07
Dy	114	21.8	114	172	227	124	134	101	128	239
Ho	24.2	6.32	40.9	60.8	78.3	38.9	42.9	31.6	42.0	91.3
Er	81.0	21.1	190	273	340	158	177	128	179	432
Tm	14.0	3.61	38.9	56.9	68.7	31.0	35.2	25.1	36.6	92.5
Yb	108	24.9	342	488	576	256	293	206	308	798
Lu	13.3	4.06	61.3	84.1	97.2	42.9	51.0	35.6	54.0	140
Hf	13777	14596	10023	11417	11260	11897	10870	11513	11324	10718
Pb	0.64	1.48	1.02	2.02	2.55	1.36	1.27	1.08	1.29	1.14
Th	17.6	6.11	30.8	36.4	55.2	43.8	42.3	39.8	43.9	40.5
U	3350	2872	479	456	495	670	370	401	454	307
Th/U	0.01	0.00	0.06	0.08	0.11	0.07	0.11	0.10	0.10	0.13
Eu/Eu* (1)	0.27	0.16		0.01	0.01	0.01	0.01	0.01	0.01	0.01
Lu/Sm (1)	7	90	222	159	133	104	83	86	116	214
Lu/Gd (1)	3	10	21	19	15	12	11	10	13	24

Eu/Eu*; 2Eu/Sm+Gd
(1); normalised to chondrite
bdl; below detection limit

vado-Filábride Complex and brittle in the Alpujárride rocks (Monié et al., 1991; De Jong, 1991), suggest this as well and agree with an earlier exhumation age for the Alpujárride rocks with respect to the Nevado-Filábride ones (Braga et al., 1996; Johnson et al., 1997).

These metamorphic and tectonic evidences, the assumption that the upper rocks of the Nevado-Filábride Complex and the lower Alpujárride units represent the same lithostratigraphic sequence, and the tectonic character of the present contact between the two complexes, had lead to the previous hypothesis that both complexes were tectonically superposed from the onset of subduction. As a consequence the contact between the two complexes was interpreted as an old thrust fault (Egeler and Simon, 1969).

However, Galindo-Zaldívar et al. (1989) and Platt and Vissers (1989) demonstrated that this contact is a late detachment normal fault formed during the extensional exhumation of the belt. This extensional normal fault appears to be responsible for the penetrative structures observed in the Nevado-Filábride Complex, and the conspicuous brittle structures of the Alpujárride Complex. This detachment also produced the increase of shear deformation in the Nevado-Filábride Complex towards the contact with the Alpujárride and the thinning perpendicular to the transposed bedding of both sequences (Jabaloy, 1991). These new data lead to a new general interpretation of the contact, according to which the extensional detachment was the reactivation of an early thrust fault (De Jong, 1991).

Taking into account the new age data of rocks, the high-pressure metamorphism, the exhumation ages of both complexes and the extensional nature of the present contact between them (see below), a question arises: are there any arguments pointing to the existence of an old thrust fault between the Nevado-Filábride and Alpujárride Complexes? On the basis of the radiometric age presented in this paper, the pressure differences of both complexes, and the progressive change in the style of the structures in the Nevado-Filábride Complex towards the extensional detachment, we propose that subduction was produced on a stratigraphic sequence in which the Nevado-Filábride Complex represents the Palaeozoic basement of the Mesozoic rocks of the lower Alpujárride units.

Age of metamorphism

The age of 16.5 ± 0.4 Ma obtained from the outer rims of the zircon crystals coincides with those determined by $^{39}Ar/^{40}Ar$ (16–17 Ma) in Nevado-Filábride white micas of the detachment zone between the Nevado-Filábride and Alpujárride Complexes for the end of metamorphism (Monié et al., 1991, Fig. 3). Even younger is the 15.0 ± 0.6 Ma age obtained from zircon from the Cerro del Almirez (Nevado-Filábride Complex, central Sierra Nevada, López Sánchez-Vizcaíno et al., 2001, Fig. 3), and from the Sierra de los Filabres (De Jong, 2003, Fig. 3), which was interpreted as dating HP metamorphism. Both ages are in conflict with the only other zircon dating published for the Nevado-Filábride rocks (Puga et al., 2003, Fig. 3). These authors attribute the Upper Cretaceous (87.4 ± 1.4 Ma) to Oligocene (30.9 ± 0.6 Ma) ages obtained in mottled zones of zircon from eclogites "to partial recrystallisation of igneous crystals during the eoalpine eclogitisation". This suggests that such ages represent a mix between igneous and metamorphic zircon. Other authors also concluded that such mottled zircon zones are unlikely to produce geologically significant ages, but rather ages intermediate between protolith crystallisation and metamorphism (Rubatto et al., 1998; Tomaschek et al., 2003).

Futher zircon ages obtained in the Betic Internal Zones were obtained from Alpujárride rocks. There is compelling evidence that these rocks reached peak metamorphism at 650–800 °C between 23 and 19 Ma (Platt et al., 1998; Platt and Whitehouse, 1999; Sánchez Rodríguez and Gebauer, 2000; Platt et al., 2003). The timing of exhumation is more controversial: Platt et al. (2003) claim that it occurred by ~18 Ma, and was synchronous over the whole area covered by the Alborán Sea and the Betic Cordillera. This conclusion is based on age determinations obtained from rocks of the Alpujárride Complex, from rocks of the Alborán Sea basement and from rocks in the Rif Chain (Platt et al., 2003), but not the Nevado-Filábride Complex. The SHRIMP age for the Sierra Nevada gneiss (16.5 ± 0.4 Ma) and previous fission track data indicating 12 and 9 Ma for final exhumation and cooling (Johnson et al., 1997), point to a younger age for the exhumation of the Nevado-Filábride Complex. Even if the age of Cerro del Almirez, Nevado-Filábride Complex, (15.0 ± 0.6 Ma; López Sánchez-Vizcaíno et al., 2001) is interpreted as dating decompression (as proposed by Platt et al., 2003) this is still significantly younger than decompression in the Alpujárride Complex (Platt et al., 2003).

In summary, despite the uncertainty in relating this and other U–Pb ages to precise metamorphic conditions, zircon data support the model of Johnson et al. (1997) of diachronous exhumation across the Betic Cordillera. In this model Nevado-Filábride and Alpujárride Complexes underwent parallel but not synchronous histories (López Sánchez-Vizcaíno et al., 2001). Diachronous HP metamorphism and exhumation has been documented in other metamorphic belts such as the Alps (Rubatto et al., 1998).

Conclusions

In the uppermost part of the Nevado-Filábride Complex (western Sierra Nevada) bodies of gneisses occur, the protoliths of which had intruded sedimentary host rocks. Fluids released from the felsic bodies produced hydrothermal processes within the contact aureole, such as replacement tourmalinites in neighbouring metapelites, veins of pegmatitic composition cutting across all of the adjacent lithologies, and skarn-like rocks near the marbles. These field occurrences demonstrate the original intrusive contact between the igneous protholith of the gneiss and the surrounding metasediments.

The U–Pb age of 301 ± 7 Ma determined in magmatic zircon cores indicates that the igneous precursor of the gneiss belongs to syn- to post-Variscan granitoids. Therefore, both the marbles and micaschists from the upper part of the Nevado-Filábride Complex are pre-Stephanian in age, rather than Triassic and Permian-Triassic respectively, as previously held. In the lower Alpujárride units of the western Sierra Nevada, Permian-Triassic phyllites and Triassic marbles are part of a normal tectono-sedimentary sequence, which overlies these Palaeozoic and older Nevado-Filábride rocks. The entire sequence is thought to have been deformed and metamorphosed under high-pressure conditions. This indicates a common evolution of both complexes from the onset of subduction. Metasediments and skarns adjacent to the gneiss yield approximate P–T conditions for this early metamorphism: 14 ± 4 kbar and 660 ± 100 °C. The age of 16.5 ± 0.4 Ma obtained from the outer rims of zircon crystals is related to decompression, as suggested by titanite inclusions, which postdate rutile, the high-pressure Ti-rich phase.

The present-day contact between the two sequences is a major low-angle normal fault generated during the extensional exhumation of the belt. This fault separates the Paleozoic rocks of the Nevado-Filábride Complex from the overlay-

ing Permian and Triassic rocks of the Alpujárride units. Consequently, sedimentological, tectonic or metamorphic arguments do not justify that the rocks above and below this extensional detachment belong to two different tectonic complexes.

Alpujárride sequences similar to those overlying the Nevado-Filábride Complex are exposed towards the W of the Betic Cordilleras on top of the so-called "Alpujárride basements". The Nevado-Filábride Complex is also the basement of Alpujárride Permo-Triassic rocks. Therefore the lithostratigraphic, tectonic and metamorphic criteria to separate both complexes need to be revised on the light of the reported new data.

Acknowledgements

This research was supported by project BTE-2000-1490-C02-01, BTE-2003-01699 (CICYT) and RNM-145 (JA). The Electron Microscopy Unit at the Australian National University is thanked for access to the SEM facility. D.R. acknowledges financial support from the Australian Research Council. We are very grateful to J.C. Braga for his comments and critical reading of the manuscript. We acknowledge the constructive comments by M. Engi and two anonymous reviewers.

References

Akkerman, J.H., Maier, G. and Simon, O.J. (1980): On the geology of the Alpujárride Complex in the western Sierra de las Estancias (Betic Cordilleras, SE Spain). *Geol. Mijnbouw* **59**, 363–374.

Angles, T.W., Prince, C.I., Foster, G.L. and Vance, D. (1999): New garnet for old? Caution tales from young mountain belts. *Earth Planet. Sci. Letters* **172**, 301–309.

Azañón, J.M. and Goffé, B. (1997): Ferro- and magnesiocarpholite assemblages as record of high-P, low-T metamorphism in the Central Alpujárrides, Betic Cordillera (SE Spain). *Eur. J. Mineral.* **9**, 1035–1051.

Bakker, H.E., De Jong, K., Helmers, H. and Biermann, C. (1989): The geodynamic evolution of the Internal Zone of the Betic Cordilleras (south-east Spain): a model based on structural analysis and geothermobarometry. *J. metamorphic Geol.* **7**, 359–381.

Barrois, C.H. and Offert, A. (1889): Memoire sur la constitution géologique du sud de l'Andalusie, de la Sierra Tejeda à la Sierra Nevada. *Mem. Acad. Sci. Nat. France* **30**, 79–167.

Belousova, E.A., Griffin, W.L., O'Reilly, S.Y. and Fisher, N.I. (2002): Igneous zircon: trace element composition as an indicator of source rock type. *Contrib. Mineral. Petrol.* **143**, 602–622.

Braga, J.C. and Martín, J.M. (1987): Distribución de las algas dasycladaceas en el Trías alpujárride. *Cuad. Geol. Iber.* **11**, 475–489.

Braga, J.C., Jiménez, A.P., Martín, J.M. and Rivas, P. (1996): Middle Miocene, coral-oyster reefs (Murchas, Granada, southern Spain). In: Franseen, E., Esteban, M., Ward, W.C., Rouchy, J.M. (Eds.): Models for Carbonate Stratigraphy from Miocene Reef Complexes of Mediterranean Regions. Concepts in Sedimentology and Paeleontology Series, SEPM, Tulsa, Oklahoma **5**, 131–139.

Brouwer, H.A. (1926): The structure of the Sierra Nevada. *Geol. Rundschau* **17**, 118–137.

Butera, K.M., Williams, I.S., Blevin, P.L. and Simpson, C.J. (2001): Zircon U–Pb dating of Early Palaeozoic monzonitic intrusives from the Goonumbla area, New South Wales. *Aust. J. Earth Sci.* **48**, 457–464.

Compston, W., Williams, I.S., Kirschvink, J.L., Zhang, Z. and Ma, G. (1992): Zircon U–Pb ages for the Early Cambrian time-scale. *J. Geol. Soc. London* **149**, 171–184.

Cuevas, J., Aldaya, F., Navarro-Vila, F. and Tubia, J.M. (1986): Caractérisation de deux étapes de charriage principales dans les nappes Alpujarrides centrales (Cordillères Bétiques, Espagne). *C. R. Acad. Sci. Paris* **302**, sér. 2, 1177–1180.

De Jong, K. (1991): Tectono-metamorphic studies and radiometric dating in the Betic Cordilleras (SE Spain). Ph.D. Thesis, Univ. Amsterdam, 204 pp.

De Jong, K. and Bakker, H. (1991): The Mulhacén and Alpujárride Complex in the eastern Sierra de los Filabres, SE Spain: Litho-stratigraphy. *Geol. Mijnbouw* **70**, 93–103.

Egeler, C.G. and Simon, O.J. (1969): Sur la tectonique de la Zone Bétique (Cordillères Bétiques, Espagne). *Verh. Kon. Ned. Akad. Wet. Natuurk.* **25**, Ser. I, 90 pp.

Eggins, S.M., Rudnick, R.L. and McDonough, W.F. (1998): The composition of peridotites and their minerals: a laser ablation ICP-MS study. *Earth Planet. Sci. Lett.* **154**, 53–71.

Fallot, P. (1948): Les Cordillères Bétiques. *Est. Geol.* **4**, 83–172.

Fallot, P., Faure-Muret, A., Fontboté, J.M. and Solé-Sabaris, L. (1961): Estudios sobre las series de Sierra Nevada y de la llamada mischungszone. *Bol. Inst. Geol. Min. España* **81**, 345–557.

Galindo-Zaldivar, J., González-Lodeiro, F. and Jabaloy, A. (1989): Progressive extensional shear structures in a detachment contact in the western Sierra Nevada (Betic Cordilleras, Spain). *Geodin. Acta* **3**, 73–85.

García-Dueñas, V., Martínez-Martínez, J.M., Orozco, M. and Soto, J.I. (1988): Plis-nappes cisaillements ductiles-fragiles en distension dans les Nevado-Filábrides (Cordillères Bétiques, Espagne). *C. R. Acad. Sci. Paris* **307**, sér. II, 1389–1395.

Goffé, B., Michard, A., Garcia-Dueñas, V., González-Lodeiro, F., Monié, P., Campos, J., Galindo-Zaldívar, J., Jabaloy, A., Martínez-Martínez, J.M. and Simancas, J.F. (1989): First evidence of high-pressure, low-temperature metamorphism in the alpujarride nappes, Betic Cordilleras (SE Spain). *Eur. J. Mineral.* **1**, 139–142.

Gómez-Pugnaire, M.T., Chacón, J., Mitrofanov, F. and Timofeev, V. (1982): First report on the Precambrian rocks in the graphite-bearing series of the Nevado-Filábride Complex (Betic Cordillera, Spain). *N. Jb. Geol. Paläont. Mh.* **3**, 176–180.

Gómez-Pugnaire, M.T. and Cámara, F. (1990): La asociación de alta presión distena + talco + fengita coexistente con escapolita en metapelitas de origen evaporítico.s Complejo Nevado-Filábride (Cordilleras Béticas). *Rev. Soc. Geol. España* **8**, 87–96.

Gómez-Pugnaire, M.T. and Fernández Soler, J.M. (1987): High-pressure metamorphism in metabasites from the Betic Cordilleras (SE Spain). *Contrib. Mineral. Petrol.* **95**, 231–244.

Gómez-Pugnaire, M.T., Franz, G. and López Sanchez-Vizcaíno, V. (1994): Retrograde formation of NaCl-scapolite in high-pressure metaevaporites from the Cordilleras Béticas (Spain). *Contrib. Mineral. Petrol.* **116**, 448–461.

Gómez-Pugnaire, M.T., Braga, J.C., Martín, J.M, Sassi, F.P. and Del Moro, A. (2000): Regional implications

of a Palaeozoic age for the Nevado-Filábride Cover of the Betic Cordillera, Spain. *Schweiz. Mineral. Petrogr. Mitt.* **80**, 45–52.

Heinrich, C. (1982): Kyanite-eclogite to amphibolite facies evolution of hydrous mafic and pelitic rocks, Adula nappe, Central Alps. *Contrib. Mineral. Petrol.* **81**, 30–38.

Helmers, H. (1982): Eclogitization of hedenbergite skarns in the Sierra de los Filabres, S.E. Spain. *Terra Cognita* **2**, 320.

Hinton, R.W. and Upton, B.G.J. (1991): The chemistry of zircon: Variations within and between large crystals from syenite and alkali basalt xenoliths. *Geochim. Cosmochim. Acta* **55**, 3287–3302.

Holland, T.J.B. and Powell, R. (1996): Thermodynamics of order-disorder in minerals. 1: symmetric formalism applied to minerals of fixed composition. 2: symmetric formalism applied to solid solutions. *Am. Mineral.* **81**, 1413–1437.

Holland, T.J.B. and Powell, R. (1998): An internally consistent thermodynamic data set for phases of petrological interest. *J. Metamorphic Geol.* **16**, 309–343.

Hoskin, P.W.O. and Black, L.P. (2000): Metamorphic zircon formation by solid-state recrystallization of protolith igneous zircon. *J. Metamorphic Geol.* **18**, 423–439.

Jabaloy, A. (1991): La estructura de la Región occidental de la Sierra de los Filabres (Cordilleras Béticas). Ph. D. Thesis, Univ. Granada, 197pp.

Johnson, C., Harbury, N. and Hurford, A.J. (1997): The role of extension in the Miocene denudation of the Nevado-Filábride Complex, Betic Cordillera (SE Spain). *Tectonics* **16**, 189–204.

Lafuste, M.J. and Pavillon, M.J. (1976): Mise en évidence d'Eifélien daté au sein des terrains métamorphiques des zones internes des Cordillères bétiques. *C. R. Acad. Sci. Paris* **283**, sér. D, 1015–1018.

López Sánchez-Vizcaíno, V., Rubatto, D., Gómez-Pugnaire, M.T., Tommsdorff, V. and Müntener, O. (2001): Middle Miocene high-pressure metamorphism and fast exhumation of Nevado-Filábride Complex, SE Spain. *Terra Nova* **13**, 327–332.

Ludwig, K.R. (2000): Isoplot/Ex version 2.4. A geochronological toolkit for Microsoft Excel. Berkeley, Berkeley Geochronological Centre Spec. Pub., 56 pp.

Martín, J.M. and Braga, J.C. (1987): Alpujárride carbonate deposits (southern Spain) – marine sedimentation in a Triassic Atlantic. *Palaeogeogr. Palaeoclimat. Palaeoecol.* **59**, 243–260.

Martínez-Martínez, J.M. (1986): Evolución tectonometamórfica del complejo Nevado-Filábride en el sector de unión entre Sierra Nevada y Sierra de los Filabres (Cordilleras Béticas). *Cuad. Geol.* **13**, 1–19.

Martínez-Martínez, J.M., Soto, J.I. and Balanya, J.C. (2002): Orthogonal folding of extensional detachments: Structure and origin of the Sierra Nevada elongated dome (Betics, SE Spain) *Tectonics* **21**, 1–22.

Monié, P., Galindo-Zaldívar, J., Goffé, B. and Jabaloy, A. (1991): First report on $^{40}Ar/^{39}Ar$ geochronology of alpine tectonism in the Betic cordilleras (southern Spain). *J. Geol. Soc. London* **148**, 289–297.

Nieto, J.M. (1996): Petrología y geoquímica de los gneisses del Complejo del Mulhacén, Cordilleras Béticas. Ph. D. Thesis Univ. Granada, 210 pp.

Nieto, J.M., Puga, E., Monié, P., Díaz de Federico, A. and Jagoutz, E. (1997): High-pressure metamorphism in metagranites and orthogneiss from the Mulhacén Complex (Betic Cordillera, Spain). *Terra Nova* **9**, abstr. supl. 1, 22–23.

Nieto, J.M., Puga, E. and Jagoutz, E. (1995): Aportacion de la geoquimica y la geocronologia de ortogneises al conocimiento de la evolucion geodinamica del complejo del Mulhacén (cordilleras Beticas, SE de España). *Bol. Soc. Esp. Mineral.* **18**, p. 79.

Nijhuis, H.J. (1964): Plurifacial Alpine metamorphism in the south-eastern Sierra de los Filabres, South of Lubrín, SE Spain. Ph. D. Thesis Univ. Amsterdam, 151 pp.

Platt, J., Soto, J.I., Whitehouse, M.J., Hurford, A.J. and Kelley, S.P. (1998): Thermal evolution, rate of exhumation, and tectonic significance of metamorphic rocks from the floor of the Alborán extensional basin, western Mediterranean. *Tectonics* **17**, 671–689.

Platt, J.P., Vissers, R.L.M. (1989): Extensional collapse of thickened continental lithosphere: a working hypothesis for the Alborán Sea and Gibraltar arc. *Geology* **17**, 540– 543.

Platt, J.P. and Whitehouse, M.J. (1999): Early Miocene high-temperature metamorphism and rapid exhumation in the Betic Cordillera (Spain): evidence from U–Pb zircon ages. *Earth Planet. Sci. Lett.* **171**, 591–605.

Platt, J.P., Whitehouse, M.J., Kelley, S.P., Carter, A. and Hollick, L. (2003): Simultaneous extensional exhumation across the Alboran Basin; implications for the causes of late orogenic extension. *Geology* **31**, 251–254.

Pidgeon, R.T., Nemchin, A.A. and Hitchen, G.J. (1998): Internal structures of zircons from Archean granites from the Darling Range batholith: implications for zircon stability and the interpretation of zircon U–Pb ages. *Contrib. Mineral. Petrol.* **132**, 288–299.

Pouchou, J.L. and Pichoir, F. (1985): PAP f(rz) procedure for improved quantitative microanalysis. In: Armstrong, J.T. (Ed.): Microbeam Analysis. San Francisco Press Inc.

Powell, R. and Holland, T.J.B. (1993): On the formulation of simple mixing models for complex phases. *Am. Mineral.* **78**, 1174–1180.

Powell, R. and Holland, T.J.B. (1994): Optimal geothermometry and geobarometry. *Am. Mineral.* **79**, 120–133.

Powell, R. and Holland, T.J.B. (1999): Relating formulations of the thermodynamics of mineral solid solutions: activity modelling of pyroxenes, amphiboles and micas. *Am. Mineral.* **84**, 1–14.

Priem, H.N.A., Boelrijk, N.A.J.M., Hebeda, E.H. and Verschure, R.M. (1966): Isotopic age determinations on tourmaline granite-gneiss and a metagranite in the Eastern Betic Cordilleras, SE Spain. *Geol. Mijnbouw* **45**, 184–187.

Proyer, A. (2003): The preservation of the high-pressure rocks during exhumation: metagranites and metapelites. *Lithos* **70**, 183–194.

Puga, E. (1976): Investigaciones petrológicas en Sierra Nevada Occidental. Ph.D. Thesis Univ. Granada, 267 pp.

Puga, E., Nieto, J.M. and Díaz de Federico, A. (2000): Contrasting P–T paths in eclogites of the Betic Ophiolitic Association, Mulhacén Complex, Southeastern Spain. *Can. Mineral.* **38**, 1137–1161.

Puga, E., Díaz De Federico, A. and Nieto, J.M. (2002): Tectonostratigraphic subdivision and petrological characterisation of the deepest complexes of the Betic zone: a review. *Geodin. Acta* **15**, 23–43.

Puga, E., Fanning, M., Nieto, J.M. and Díaz de Federico, A. (2003): Datación U–Pb con SHRIMP de circones de las eclogitas ofiolíticas del Complejo del Mulhacén (Cordillera Bética). *Geogaceta* **33**, 131–134.

Rubatto, D., Gebauer, D. and Fanning, M. (1998): Jurassic formation and Eocene subduction of the Zermatt-Saas-Fee ophiolites: implications for the geodynamic evolution of the Central and Western Alps. *Contrib. Mineral. Petrol.* **132**, 269–287.

Rubatto, D. and Hermann, J. (2003): Zircon formation during fluid circulation in eclogites (Monviso, Western Alps): implications for Zr and Hf budget in subduction zones. *Geochim. Cosmochim. Acta* **21**, 833–852.

Sánchez-Rodríguez, L. and Gebauer, D. (2000): Mesozoic formation of pyroxenites and gabbros in the Ronda area (southern Spain), followed by Early Miocene subduction metamorphism and emplacement into the middle crust: U–Pb sensitive high-resolution ion microprobe dating of zircon. *Tectonophysics* **316**, 19–44.

Schönbächler. M. (1999): Die Hochdruckmetamorphose der Ultramafika und der angrenzenden Nebengesteine am Cerro de Almirez, Sierra Nevada, Südspanien. Teil I. Unpublished Diplomarbeit, ETH, Zürich, 113 pp.

Soto, J.I. (1993): Estructura y evolución metamórfica del Complejo Nevado-Filábride en la terminación oriental de la Sierra de los Filabres (Cordilleras Béticas). Ph. D. Thesis Univ. Granada, 270 pp.

Staub, R. (1934): Der Deckenbau Südspaniens in den Betischen Cordilleren. *Vierteljahresschrift Naturf. Ges. Zürich* **79**, 271–332.

Tendero, J.A., Martín-Algarra, A., Puga, E. and Diaz de Federico, A. (1993): Lithostratigraphie des métasédiments de l'association ophiolitique Nevado-Filábride (SE Espagne) et mise en évidence d'objets ankéritiques évoquant des foraminifères du Crétacé: conséquences Palèogéographiques. *C.R. Acad. Sci. Paris* **316**, sér. II, 1115–1122.

Tomaschek, F., Kennedy, A.K., Villa, I.M., Lagos, M. and Ballhaus, C. (2003): Zircons from Syros, Cyclades, Greece – Recrystallization and mobilization of zircon during high-pressure metamorphism. *J. Petrol.* **44**, 1977–2002.

Torres-Roldan, R.L. (1979): The tectonic subdivision of the Betic Zone (Betic Cordilleras, southern Spain); its significance and one possible geotectonic scenario for the westernmost Alpine Belt. *Am. J. Sci.* **279**, 19–51.

Torres-Ruiz, J., Pesquera, A., Gil-Crespo, P.P. and Velilla, N. (2003): Origin and petrogenetic implications of tourmaline-rich rocks in the Sierra Nevada (Betic Cordillera, southeastern Spain). *Chem. Geol.* **197**, 55–86.

Trommsdorff, V., López-Sánchez Vizcaíno, V., Gómez-Pugnaire, M.T. and Müntener, O. (1998): High pressure breakdown of antigorite to spinifex-textured olivine and orthopyroxene, SE Spain. *Contrib. Mineral. Petrol.* **132**, 139–148.

Tubia, J.M. and Gil-Ibarguchi, J.L. (1991): Eclogites of the Ojen Nappe; a record of subduction in the Alpujarride Complex (Betic Cordilleras, southern Spain). *J. Geol. Soc. London* **148**, 801–804.

Vissers, R.L.M. (1981): A structural study of the central Sierra de los Filabres (Betic Zone, SE Spain). GUA Papers of Geology. Ser.1, 15, 154 pp.

Voet, H.W. (1967): Geological investigations in the northern Sierra de los Filabres around Macaél and Cóbdar south-eastern Spain. Ph.D. Univ. Amsterdam, 122 pp.

Westra, G. (1969): Petrogenesis of a composite metamorphic facies series in a intricate fault-zone in the SE Sierra Cabrera, SE Spain. Ph.D. Thesis, Univ. Amsterdam, 143 pp.

Whitehouse, M.J. and Kamber, B.S. (2002): On the overabundance of light rare earth elements in terrestrial zircons and its implications for Earth's earliest magmatic differentiation. *Earth Planet. Sci. Lett.* **204**, 333–346.

Whitehouse, M.J. and Platt, J.P. (2003): Dating high-grade metamorphism constraints from rare earth elements in zircon and garnet. *Contrib. Mineral. Petrol.* **145**, 61–74.

Received 5 February 2004
Accepted in revised form 12 April 2005
Editorial handling: M. Engi